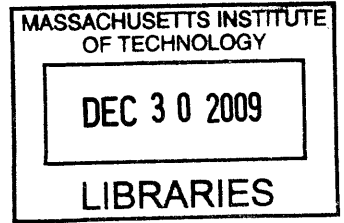


Study on Mechanical Properties of Cork Composites in a Sandwich Panel for Wind Turbine Blade Material

by

Sungmin Kim

B.S. Mechanical Engineering
Seoul National University, 2006



SUBMITTED TO THE DEPARTMENT OF MECHANICAL ENGINEERING IN PARTIAL FULFILLMENT OF THE REQUIREMENTS FOR THE DEGREE OF

MASTER OF SCIENCE IN MECHANICAL ENGINEERING
AT THE
MASSACHUSETTS INSTITUTE OF TECHNOLOGY

ARCHIVES

JUNE 2009

© 2009 Massachusetts Institute of Technology. All rights reserved.

The author hereby grants to MIT permission to reproduce and to distribute publicly paper and electronic copies of this thesis document in whole or in part in any medium now known or hereafter created.

Signature of
Author

Department of Mechanical Engineering
May 22, 2009

Certified
by

David Wallace
Professor
Thesis Supervisor

Accepted
by

Dave E. Hardt
Chairman, Department Committee on Graduate Students

Study on Mechanical Properties of Cork Composites in a Sandwich Panel for Wind Turbine Blade Material

By

Sungmin Kim

Submitted to the Department of Mechanical Engineering
on 22 May 2009, in partial fulfillment of the requirements
for the degree of Master of Science in Mechanical Engineering

Abstract

Wind energy has become one of the most promising energy sources due to its environmentally friendliness, unlimited amounts. To become competitive energy source among other sustainable and clean energy, such as solar cell, tidal energy, the price to produce the wind energy should drop and stable energy supply should be achieved. In the components of wind turbine, the highest cost item is rotor blades. The study on rotor blades material has been conducted globally in order to find cheaper materials without significant performance defects. The most widely used material for manufacturing rotor blades is glass reinforced plastic (GRP) these day, but in terms of being green technology, GRP does not satisfy all our environmental concerns.

The cork is a raw material of great value for the country whose economy is strongly bonded to cork industry. It has excellent properties such as low density, high energy absorption, low thermal conductivity, and water tightness. However, its application has been restricted to some traditional sectors such as bottle stoppers, not having reached all of its potential use. In this study, using sandwich structures, the possibility of cork core composites as a rotor blade material has been explored by determining its mechanical properties. In order to compare the mechanical properties of GRP, fiberglass laminates samples are also made and tested.

Thesis Supervisor: David Wallace

Title: Professor of Mechanical Engineering

Acknowledgements

First of all, I would like to appreciate my advisor Prof. David Wallace for giving me a great chance to become his student and work with him. I really enjoyed my research and life here due to his significant support during my master's journey.

I thank my lab mates, Barry Kudrowitz, James Penn, and Sunyoung, and would like to express special thankful mind to Sangmok Han who rescued my life tons of time in MIT and led me to MIT Korean Class which gives me an amazing experience. I also appreciate my precious friends, Kyunghye Kim, Jongsup Hong, Hanbee Na, Yun Seog Lee, Hansohl cho, Yunna Sinsky, Yongdae Shin, Sangwon Byun, Jessie Jeon, who made my life here amazingly joyful. I am very grateful to Pierce Hayward to let me use the lab and give me great help, and Connie Yeh to help me out from the very beginning of research.

Especially I would like to give my gratitude to my family. Without their endless love and support, I would not be here.

This project was supported by MIT-Portugal Program.

Contents

1. Introduction.....	14
1.1. Motivation.....	14
1.2. Current Challenges.....	16
1.3. Cork.....	17
1.4. Objective.....	17
2. Experiments and Results.....	19
2.1. Background.....	19
2.1.1. Overview of Wind Turbines.....	19
2.1.2. Functional Requirements	27
2.1.3. Limitations on Existing Materials.....	30
2.2. An Alternative Design Proposal.....	31
2.2.1. A Sandwich Structure with Cork Core Composites.....	31
2.2.2. Sandwich Structures.....	32
2.2.2.1. Core Materials.....	33
2.2.2.1.1. Honeycomb.....	33
2.2.2.1.2. Foam.....	34
2.2.2.1.3. Balsa.....	34
2.2.2.2. Skins.....	35
2.3. Designing and Manufacturing Samples	36
2.3.1. Sandwich Panels with Cork Core.....	36
2.3.1.1. Manufacturing Procedure.....	37
2.3.1.2. Design Parameter Variations.....	39
2.3.1.2.1. Sizes of Cork Granules	39
2.3.1.2.2. Amount of Epoxy.....	41
2.3.1.2.3. Additional Fiberglass fillers.....	45

2.3.1.2.4.	Skins	46
2.3.2.	Glass Reinforced Plastic (GRP).....	47
2.3.2.1.	Manufacturing Procedure.....	48
2.3.2.2.	Design Parameter Variations.....	51
2.4.	Evaluation of Properties.....	52
2.4.1.	Strength.....	52
2.4.1.1.	Bending Test.....	52
2.4.1.1.1.	Background Theory	52
2.4.1.1.2.	Experimental Setup.....	57
2.4.1.1.3.	Results and Analysis.....	59
2.4.1.2.	Tensile Test.....	71
2.4.1.2.1.	Background Theory.....	71
2.4.1.2.2.	Experimental Setup.....	73
2.4.1.2.3.	Results and Analysis.....	75
2.4.1.3.	Charpy V-notch Test.....	84
2.4.1.3.1.	Background Theory.....	84
2.4.1.3.2.	Experimental Setup.....	86
2.4.1.3.3.	Results and Analysis.....	87
2.4.1.4.	Conclusion.....	89
2.4.2.	Damping Properties.....	90
2.4.2.1.	Sound Attenuation.....	90
2.4.2.1.1.	Background Theory.....	90
2.4.2.1.2.	Experimental Setup.....	92
2.4.2.1.3.	Results and Analysis.....	93
2.4.2.2.	Dynamic Mechanical Analysis.....	95
2.4.2.2.1.	Background Theory.....	95
2.4.2.2.2.	Experimental Setup.....	97

2.4.2.2.3.	Results and Analysis.....	98
2.4.2.3.	Conclusion.....	101
2.4.3.	Isolation Properties.....	102
2.4.3.1.	Thermal Conductivity	102
2.4.3.1.1.	Background Theory.....	102
2.4.3.1.2.	Experimental Setup.....	104
2.4.3.1.3.	Results and Analysis.....	108
3.	Conclusion.....	110
3.1.	Summary.....	110
3.1.1.	Advantages.....	110
3.1.2.	Limitations.....	111
3.2.	Other Applications.....	111
3.3.	Future Work.....	112

List of Figures and Tables

- Figure 1.1 Wind Turbines
- Figure 1.2 U.S national capacity growth of wind energy system
- Figure 2.1 Cross section of a rotor blade
- Figure 2.2 Wind flow and loads on a wind turbine
- Figure 2.3 How a wind turbine works
- Figure 2.4 The swept area of rotor blades
- Figure 2.5 Wind turbine power curve
- Figure 2.6 Generated wind power versus tower height
- Figure 2.7 Diagram showing stiffness versus density of material
- Figure 2.8 A sandwich panel under bending load
- Figure 2.9 Honeycomb as a core material
- Figure 2.10 Light foam as a core material
- Figure 2.11 Balsawood as a core material
- Figure 2.12 Vacuum bag setup
- Figure 2.13 Cross section diagram of the vacuum bag setup
- Figure 2.14 The biggest cork granules: 4-5mm
- Figure 2.15 The medium size of cork granules: 2-3mm
- Figure 2.16 The finest cork granules: 1mm
- Figure 2.17 Epoxy sneaked out through molds
- Figure 2.18 A cork composite with less epoxy
- Figure 2.19 A cork composite with resin at 1:2 ratio of cork to epoxy by volume
- Figure 2.20 Cork granules with short fibers
- Figure 2.21 Cork granules with long fibers
- Figure 2.22 A one sided cork composite
- Figure 2.23 Randomly Oriented fiberglass mat
- Figure 2.24 Fiberglass cloth for a skin
- Figure 2.25 Ten layers of fiberglass mats wetted through epoxy on the bottom mold

Figure 2.26 Fiberglass sample

Figure 2.27 A fiberglass specimen for bending test

Figure 2.28 A beam undergoing a three-point bending load

Figure 2.29 Display of coordinate system on a beam

Figure 2.30 A sandwich structure cross section: e_p and e_c indicate the thickness of skin and core respectively

Figure 2.31 Bending test setup

Figure 2.32 A sandwiched cork specimen for bending test

Figure 2.33 Flexural modulus of pure cork composites

Figure 2.34 Flexural strength of pure cork composites

Figure 2.35 Flexural modulus of cork composites with long fibers

Figure 2.36 Flexural strength of cork composites with long fibers

Figure 2.37 Flexural modulus of cork composites with short fibers

Figure 2.38 Flexural strength of cork composites with short fibers

Figure 2.39 Core cork with short fibers and epoxy

Figure 2.40 Core cork with long fibers and epoxy

Figure 2.41 The graph of one sided cork composite from bending test

Figure 2.42 The graph of sandwiched cork composites from bending test

Figure 2.43 The graph one sided fiberglass samples from bending test

Figure 2.44 The graph of sandwiched fiberglass samples from bending test

Figure 2.45 The density versus flexural modulus for tested samples

Figure 2.46 The density versus flexural strength for tested samples

Figure 2.47 Ashby chart showing where the flexural modulus of samples are located

Figure 2.48 Ashby chart showing where the flexural strength of samples are located

Figure 2.49 Bar carrying tensile load P

Figure 2.50 Elongation of the bar caused by force

Figure 2.51 Tensile test setup

Figure 2.52 Dimension of tensile specimen

Figure 2.53 A tensile specimen

Figure 2.54 Tensile modulus of pure cork composites

Figure 2.55 Tensile strength of pure cork composites

Figure 2.56 Tensile modulus of composites with(short, long)/without fibers

Figure 2.57 Tensile strength of cork composites with(short, long)/without fibers

Figure 2.58 Tensile modulus of fiberglass and cork composites with skin and fibers

Figure 2.59 Tensile strength of fiberglass and cork composites with skin and fibers

Figure 2.60 the density versus tensile modulus for tested samples

Figure 2.61 the density versus tensile strength for tested samples

Figure 2.62 Ashby chart showing where the flexural and tensile modulus of samples are located

Figure 2.63 Ashby chart showing where the flexural and tensile strength of samples are located

Figure 2.64 Dimensions of charpy testing apparatus

Figure 2.65 A Notched specimen for charpy test

Figure 2.66 Apparatus for the charpy V-notch test

Figure 2.67 A V-notched specimen for charpy test

Figure 2.68 The density versus impact resistance

Figure 2.69 Noise levels of various sounds

Figure 2.70 The apparatus for sound attenuation test in the booth

Figure 2.71 The apparatus to make sound by hitting a sample with a wood piece

Figure 2.72 PRAAT program to analyze the sound property

Figure 2.73 The response of a perfect elastic and viscous material for sinusoidal force

Figure 2.74 Modulus vectors

Figure 2.75 Dynamic mechanical analyzer Q800

Figure 2.76 Tan delta of each samples versus frequency

Figure 2.77 The density versus tan delta (damping) of various materials

Figure 2.78 heat conduction between two heat sources

Figure 2.79 Schematic of LFA 457*MicroFlash*®

Figure 2.80 LFA 457*MicroFlash*®

Figure 2.81 A cork specimen for thermal conductivity test

Figure 2.82 A cork specimen after graphite spraying

Figure 2.83 Furnace of LFA 457

Table 2.1 Fiber volume fraction in different process

Table 2.2 The results of bending test showing the strongest cork combination

Table 2.3 The results of bending test showing the strongest cork combination with long fibers

Table 2.4 The results of bending test showing the strongest cork combination with short fibers

Table 2.5 The results of bending test

Table 2.6 The results of tensile test showing the strongest cork combination

Table 2.7 The results of tensile test showing the strongest cork combination

Table 2.8 The results of tensile test

Table 2.9 The impact resistance per thickness of specimens

Table 2.10 The toughness of specimens

Table 2.11 The results from the sound attenuation test

Table 2.12 The damping and viscous damping ratio of each samples

Table 2.13 The viscous damping ratio of various system for comparison

Table 2.14 The results of thermal conductivity test

Table 2.15 The thermal conductivity of other materials

1. Introduction

1.1 Motivation

Historically, natural energy resources such as wood, coal, oil and natural gas have supplied the energy. However, the problem is that these natural energy resources have limited storage on earth. Due to enlarged civilization and increasing population globally, we are facing the serious problem of energy resources exhaustion. Renewable energy resources are have been suggested as the solution to this global energy issue[1]. There is another rising issue on using energy: pollution of the world. When we burn the natural resources in order to supply energy as a form of electricity, chemically harmful and environmentally malignant gases are generated inevitably. This issue has led to the focus on the paradigm of sustainable energy, which is environmentally friendly and is abundant. To meet the increased energy demands all over the world as well as environmental concern, characteristics, usability and cost of many different types of sustainable energy have been explored.



Figure 1.1 Wind Turbines [2]

Wind Energy is one of the most promising future energy resources among sustainable energy due to its environment-friendliness, unlimited amount and low cost. Wind energy does not generate any hazardous waste nor consume natural resources such as coal, oil, or gas in order to produce electricity. Recognition of the value of wind energy has triggered rapid growth in wind energy power systems all over the world; there has been higher than 30% increment yearly since 1994 [3]. In 2009, a total power of 8,500 MW was installed and this made wind power generating capacity in the United States stand at 25,369 MW, supplying sufficient electricity to power the equivalent of close to 7 million households[4]. Energy supplied by the wind energy system is expected to take up to 15 % of the total amount of generated electricity eventually. The rapid growth in wind power system establishment is expected to continue and speed up globally.

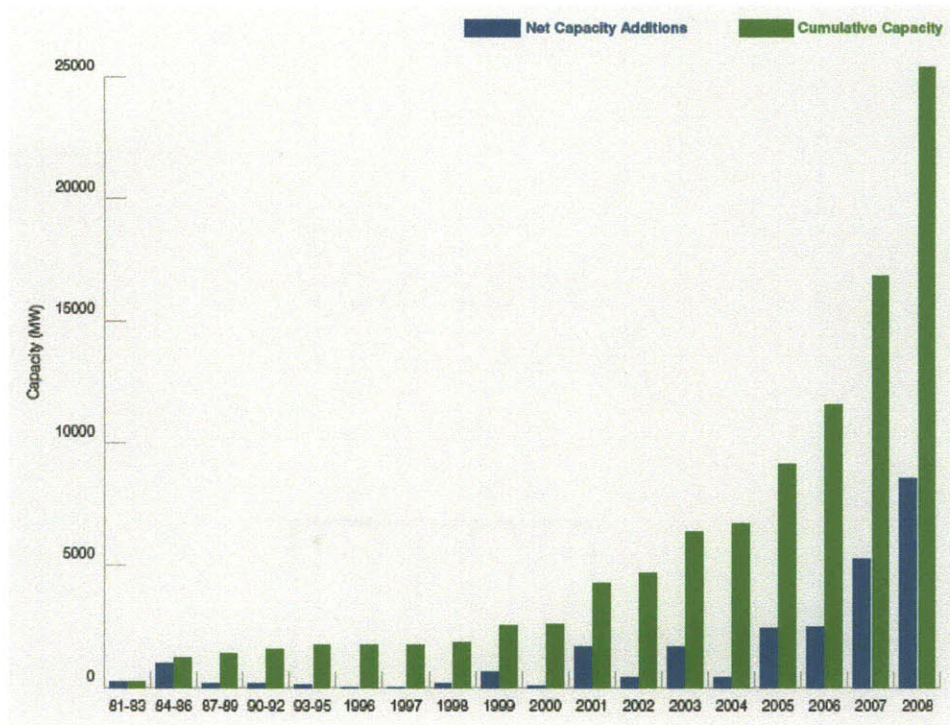


Figure 1.2 U.S national capacity growth of wind energy system [4]

1.2 Current Challenges

As the wind power system industry is growing bigger, more research on wind turbines has been conducted to improve their performance and efficiency and reduce the cost to manufacture them. The essential component to making wind energy competitive among other clean energy resources is weight and cost of wind turbines. While ensuring maintenance of the reliability of performance quality, developing low cost and high volume production material for wind turbine is the key to make the wind energy more attractive. The most effective way to cut down the cost for manufacturing wind turbines is to develop low cost material for the highest cost item in the wind turbine components

which is rotor blades(20-30% of machine cost)[3]. Therefore, study on materials for rotor blades of wind turbine has been carried out as well.

1.3 Cork

Cork is a natural product obtained from the outer bark of the cork oak. It is light and does not absorb water. It also has very low thermal conductivity which makes it a good insulator, and has excellent energy-absorbing capacity. Due to its elasticity and impermeability cork is mostly used as a bottle stoppers, especially for wine bottles. Using Cork as stoppers for bottles is one of the traditional ways to consume cork and it still takes about 60% of all cork based production[5],[6]. Its applications have been restricted to traditional sectors, not having reached all of its potential use. Development of new cork materials in composites has been studied to use its good properties for other applications. Space vehicles or complex structures under vibration and dynamic loads are examples of their high-tech applications[6].

1.4 Objective

This study aims to explore the possibility for cork as a new material for rotor blade of wind turbines by determining its mechanical properties. We decided to choose cork as filler in a glass fiber-reinforced plastic core of a sandwich panel for rotor blades of wind turbine since cork itself is weak material. Different types of cork composites are made and tested to determine its mechanical properties to explore its potential possibility as a core material in a sandwich panel. In this study, vacuum molding method is used to

make samples for tests, but in order to make real size rotor blades different ways of manufacturing should be invented. Therefore, Actual wind turbine manufacturing using cork is a remaining future work.

2. EXPERIMENTS AND RESULTS

2.1 Backgrounds

2.1.1 Overview of Wind Turbines

The power contained in wind can be converted into electricity by rotor blades with an aerodynamic shape to be able to rotate[8]. Even wind turbines have many sizes and configurations and are made from broad range of materials, they mainly consist of rotor that has wing shaped blades mounted to a hub; a nacelle that covers a drivetrain consisting of a gearbox, connecting shafts, the generator, and a tower[3].

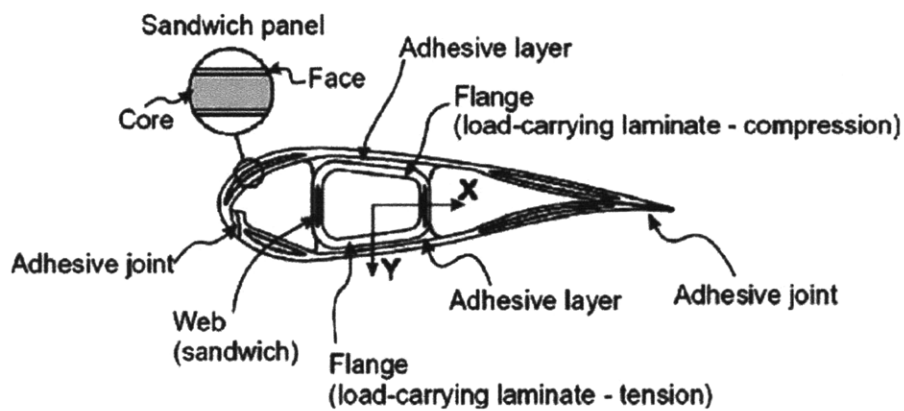


Figure 2.1 Cross section of a rotor blade [1]

Figure 2.1 shows how a rotor blade cross section looks like. Relatively thin shell outside forms the outer contour of airfoil. A longitudinal beam which is called web supports outer shell and also carries the force acting on its shell when rotating. To reduce unnecessary weight of a rotor blade, it is tapered along the longitudinal direction. It is also twisted in order to improve aerodynamic efficiency[8].

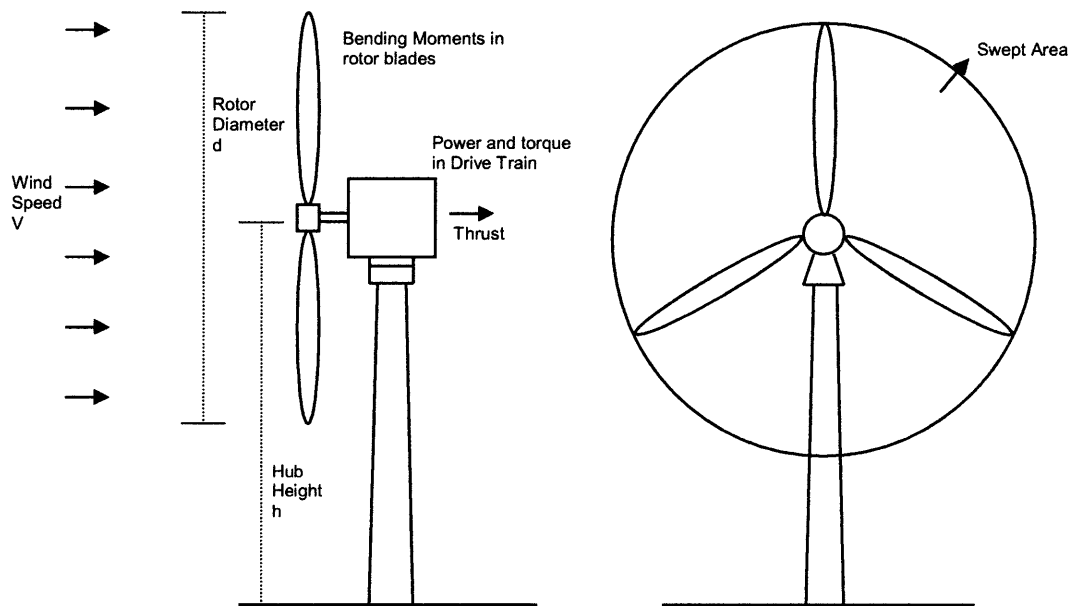


Figure 2.2 Wind flow and loads on a wind turbine

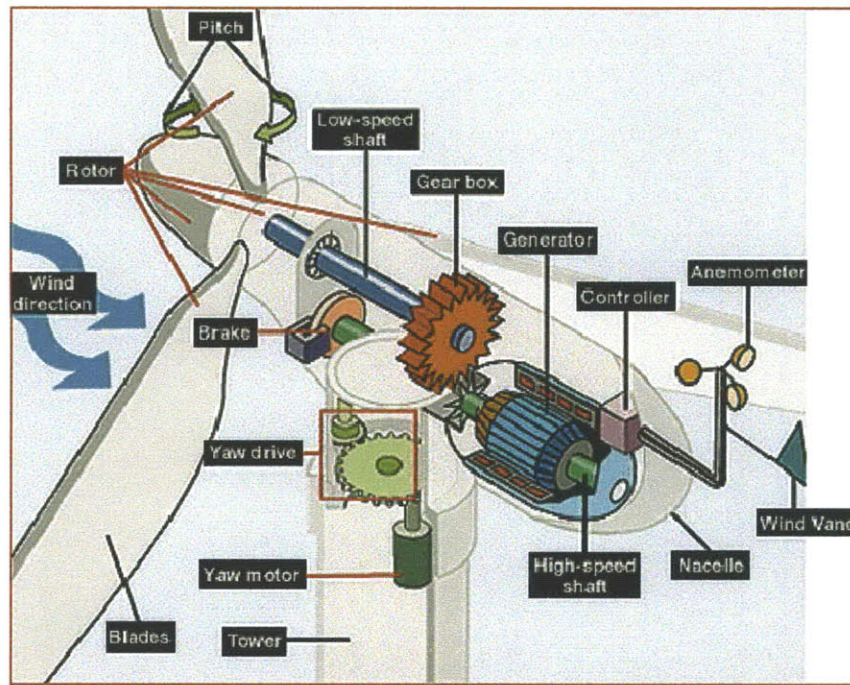


Figure 2.3 How a wind turbine works [8]

The principle of generating electricity from wind turbines is simple: After passing over the blades, wind starts exerting turning force on them. The rotating blades make a shaft turn which is inside nacelle, and this turning shaft delivers the torque to a gear box. The rotation speed should be increased for generator to convert the rotational energy into electrical energy by using magnetic field because usual rotation speeds of rotor blades are 5-20 rpm (revolution per minute) and electrical speeds in generator are 750-3600 rpm [10][11].

The formulas for calculating power from wind turbine are:

$$P_w = 1/2 \rho A V^3 \quad (1)$$

$$P_e = k C_p 1/2 \rho A V^3 \quad (2)$$

Where

P_w = Power in the wind flow through the rotor of swept area A ;

P_e = Electrical power output of the generator;

ρ = Density of air;

A = Swept area;

V = Wind speed;

$k = 0.000133$ A constant to yield power in kilowatts;

(Multiplying the above kilowatt answer by 1.340 converts it to horse- power [i.e., 1 kW = 1.340 horsepower]) [12] and

C_p = Power conversion coefficient of the rotor, ranging from 0.25 to 0.45.

(Theoretical maximum = 0.59)

The size of rotor blades tends to increase over the years. The reason is that bigger the swept area(A) rotor blades have, more available energy can be harvested from the wind that captured by rotor blades as more wind deliver the more energy (see equation(1),(2)).

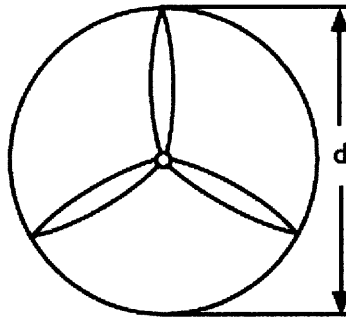


Figure 2.4 The swept area of rotor blades

The area that a rotor covers when it rotates is called the swept area. The formula for calculating swept area is

$$A = \pi r^2 = \pi (1/2d)^2 \quad (3)$$

Where

r = radius of the circular disc = ½ diameter (d)

As we've seen from equation (1), the power that we can extract from the wind is a function of the cube of the wind speed. If wind speed becomes double, its energy content will increase eight-fold. Wind Turbines that placed where the average wind speed is 8m/s produce almost 75-100% more electricity than those where the average wind speed is 6m/s. Most wind turbines start producing electricity at wind speeds of 3-4 m/s, (8 miles per hour), generate maximum 'rated' power at 15 m/s (30mph), and shut down at 25 m/s or above (50mph) to avoid storm damage on itself while operating[11].

Wind blows faster in higher altitude because of friction between wind and obstacles such as trees, buildings and geometry effect at lower altitude. The change of velocity with altitude is called 'wind shear'. The wind speed is proportional to the seventh root of altitude. If altitude becomes double then wind speed will be increased by 20%-60%[11].

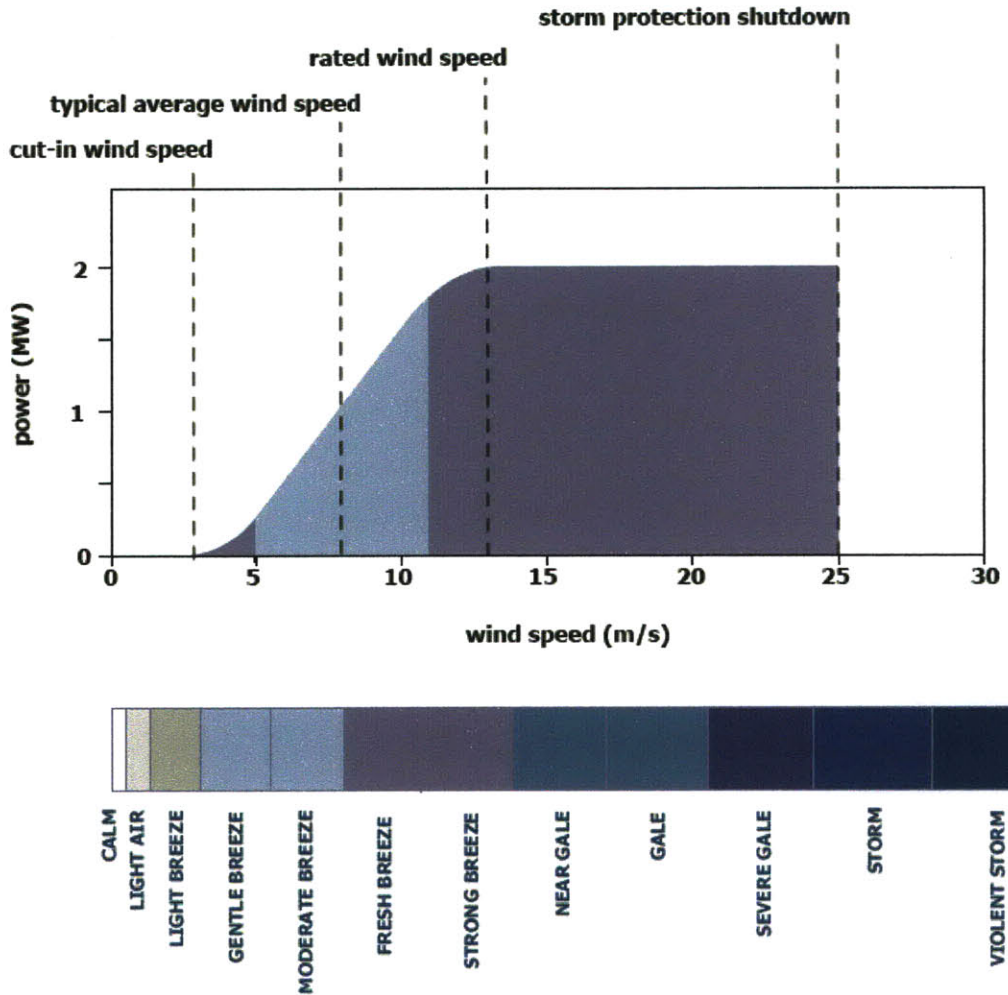


Figure 2.5 Wind turbine power curve[9]

Wind Speeds Increase with Height

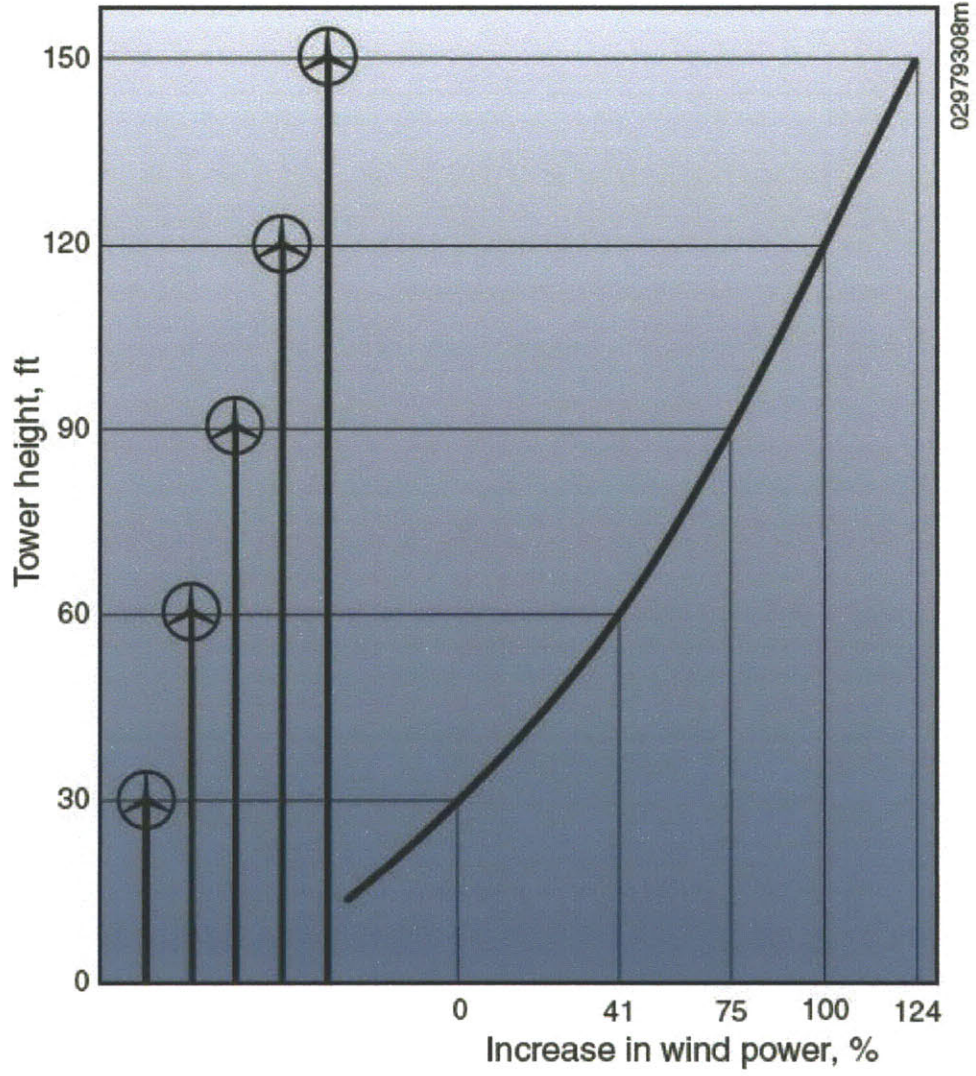


Figure 2.6 Generated wind power versus tower height [11]

The ratio of the blade tip speed and the wind speed (V) which is called tip speed ratio is also an important factor for wind turbines. When the ratio is almost 1 which means the blade tip speed and the wind speed is almost same, it is said that a wind turbine rotates slowly. If the tip speed is several times faster than the wind speed it rotates quickly. For high efficiency 3 blades turbines this ratio is in the range of 6-10[12]. This number is determined as airfoil of a rotor blade is designed.

$$rpm = V(\text{Tip speed ratio})60 / 2\pi r \quad (4)$$

$$v_T = \frac{2\pi r}{T} \quad (5)$$

Where

V= wind speed;

v_T = wing tip speed;

R= radius of the circular disc (see figure);

T= time taken for a wing tip to travel one circle circumference $2\pi r$

Wing tip speed (v_T) increases with size of rotor blades at a constant operating rpm. Large rotors usually have a lower rotational speed than small rotors to end up with the same tip speed [11],[12].

2.1.2 Functional Requirements

In this study, we mainly focus on rotor blades of wind turbines and even more specifically materials for rotor blades.

A rotor blade is exposed to gravity, centrifugal force, aerodynamic forces such as lift and drag. Therefore, in wind turbine design and material choice, material fatigue properties are considered as an important factor due to its 20-30 years of life and at least order of 10^8 fatigue stress cycles[3]. This imposes that materials for wind turbine should be strong and stiff.

Wind power generation is often considered as a non reliable resource since wind does not blow continuously. Therefore, the survey for wind power generation system location should be conducted in advance. In order to maintain stable power supply at the installed location it should be controlled precisely to maximize its output at the varying wind speed by keeping up the designed tip speed ratio. If a rotor blade is made of light density materials such as composites it can accelerate quickly to pick up blowing wind in order to keep the designed tip speed ratio. The size of wind turbines tends to get bigger to generate more energy. However, bigger size of a rotor blade always accompanies heavier weight in itself and eventually structural buckling. That is the reason why light materials such as composite are mostly used for rotor blades construction.

Corrosion resistance and breaking toughness rigidity also affect the material selections as well.

The material requirements for rotor blades materials can be summarized with high stiffness, low weight, and long fatigue life. The design of a rotor blade can be considered as a design of a beam, and merit index for this case is

$$M_b = E^{1/2} / \rho \quad (6)$$

Where

E = Young's Modulus, and

ρ = Density

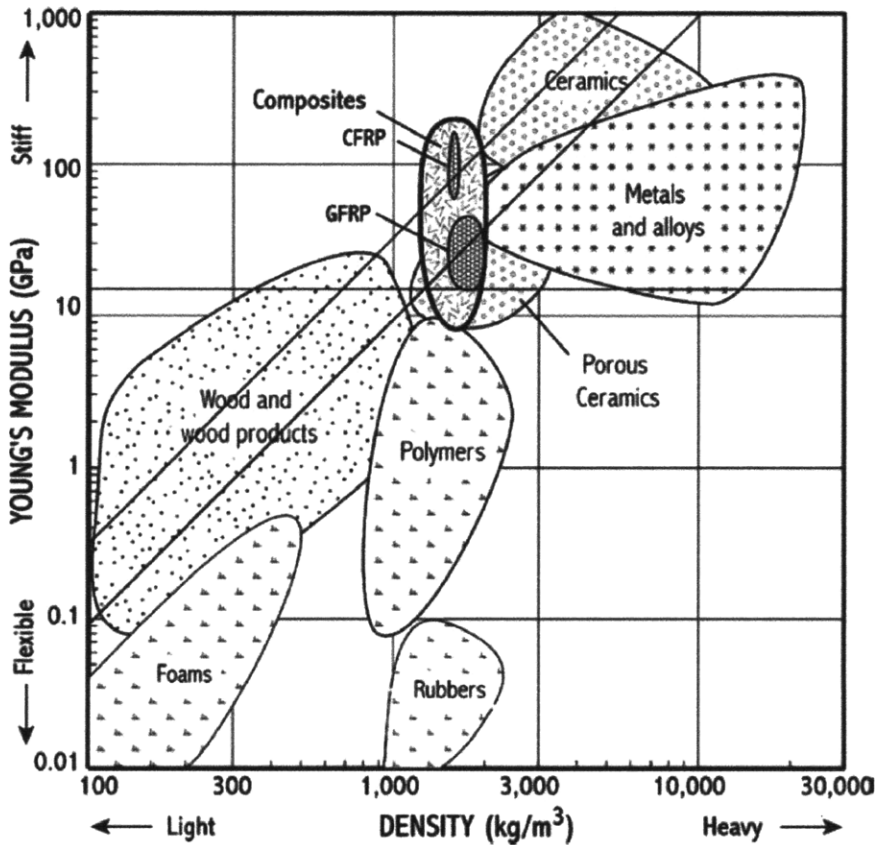


Figure 2.7 Diagram showing stiffness versus density of material [1]

Figure 2.7 schematically shows that which materials are suitable for a cantilever beam in terms of stiffness and density. The merit of lower line is 0.003 with units of E in GPa and ρ in kg/m^3 . The proper materials for the merit with 0.003 are woods, composites, porous ceramics, metals, and ceramics. The upper line which corresponds to merit with 0.006 shows that woods, composites, and ceramics are candidate materials[1]. Along the line of M_b the nominal value of E versus density is the same. The bigger number of E_b at the same density value implies that the materials whose density is smaller than other materials are more attractive for light structure construction. That shows how woods, composites such as GRP and CFRP become candidate materials for rotor blades of wind turbine.

Second criterion for rotor blades materials is stiffness on an absolute scale. Two different deflections on rotor blades occur when it rotates one circle. In order to stand order of 10^8 revolutions and $2 \cdot 10^8$ of deflections occurred during the life time of rotor blades, the limit for stiffness should be set up at relatively high number of stiffness. The suggested range of stiffness by reference [1] is 10-20GPa. The horizontal line in figure 2.7 indicates that materials on or above 15GPa satisfy second criterion. According to this criterion, most woods are not strong enough for rotor blades. That is the reason why composite materials have been dominantly used for rotor blades. In large turbines rotor blades which need stiff and strong materials are usually made out of glass reinforced plastic (GRP), and small turbines which needs relatively less stiffness materials are made out of wood-epoxy.

2.1.3. Limitations of Existing Materials

A wide range of materials have been used in wind turbines. Composite structures are often preferred over homogenous materials for their increased strength and stiffness per weight, excellent vibration damping and fatigue resistance[13],[14]. Most rotor blades in use are made from glass fiber-reinforced-plastic (GRP), i.e. glass fiber-reinforced-plastic with polyester or epoxy[3]. Carbon filament- reinforced-plastic (CFRP) is also used because it has even better material properties than GRP. However, carbon fibers are electrical conductors, so contact with metal may lead to corrosion[15]. Also high cost restricts its wide use for structure. Woods are potentially interesting because of their low density and excellent fatigue properties and environmentally friendliness, so more developments are still going on. Since it is quite weaker than GRP/ CFRP and controlling the quality of woods during processing for rotor blade structure is difficult because of its own natural structure, woods are used for relatively small wind turbine[3],[8]. Other materials have been tried include aluminum, steel, and various composites[3]. However, steel is too heavy and aluminum does not have good metal fatigue, so these make them less attractive to use as rotor blades materials.

GRP/CFRP composes rotor blades in the form of laminates. In order to make composite laminates, all layers should be laid up and wetted through with resin to be saturated perfectly in the wing shape mold by hands. Vacuum is also applied to eliminate the air bubbles inside the fabrics for few hours. The time needed to be under the pressure depends on what you choose to use a matrix. Then whole material is polymerized under the pressure. This is so labor intensive and costly[16].

The most challenging part on study for rotor blades is to find the optimum design point among properties, performance, and economy[1]. Even small alteration of the profile shape changes the power curve and noise level very dramatically, so selection of profile shape of a rotor blade should be very careful and based on past experience. Different airfoils show different aerodynamic properties. For some airfoils the power curve is better at low and middle range of wind speed and drops at high wind speed. Therefore, before constructing wind power system, the climate and blowing wind characteristics at the site where they are constructed should be surveyed to choose suitable profile shape[8]. Since the highest cost item in wind turbines is rotor blades as we mentioned above, if we could develop materials that are not only strong , stiff and light but also cheaper than general materials for rotor blades that meet as many as requirements of wind turbine performance it should be the best solution.

2.2 An Alternative Design Proposal

2.2.1 A Sandwich Structure with Cork Core Composite

A sandwich panel is often used structure in a rotor blade construction. Outer contour of airfoil shape is often constructed with sandwich structure due to its low density and high stiffness as seen in the figure 2.1. Its excellent properties with light density have made us consider it as a candidate structure for constructing rotor blades. For the core material, we select the cork composites due to its light density, excellent impact absorption and good isolation properties. Therefore, in this study we have explored cork composite core in a sandwich panel for wind turbine rotor blades. First of all, study on sandwich structures is needed.

2.2.2 Sandwich Structures

Sandwich panels are widely used in construction these days because its idea is very appropriate for lightweight structures such as aerospace structures due to extremely high in-plane and flexural stiffness to weight ratios. A sandwich panel, one of special type of laminate, typically consists of two thin facing materials (skins) and lightweight, thicker and low-stiffness core materials. The facing materials are diverse. Composite laminates and metals are typical facing materials. Composite materials including metallic or nonmetallic honeycomb, foam, and woods are examples of light materials used in sandwich panels as core materials[16],[17]. The advantages of using sandwich panels in structures are due to its lightweight compared to its high flexural rigidity. Another attractive part of using sandwich panels is that core materials can be designed to meet the specific requirements for structures. One of the disadvantages of using sandwich structure is that sandwich materials are not dampening which means it has no acoustic insulation,[16]. Figure 2.8 shows a sandwich panel under a bending load.

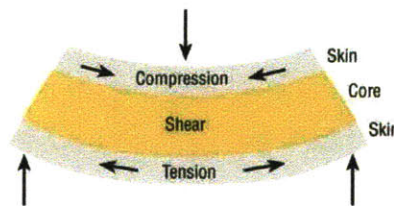


Figure 2.8 A sandwich panel under bending load [17]

2.2.2.1 Core Materials

The flexural stiffness of a sandwich panel is determined by its thickness which is contributed by core thickness. Because the flexural stiffness of any panel is proportional to the cube of its thickness, stiffness of a sandwich panel can be increased by thickening it with a low-density core material. By adding little weight on core, the laminates can obtain a huge increase in stiffness[17].

2.2.2.1.1 Honeycomb

Honeycombs are made of hexagonal cells regularly spaced[17]. For low strength and stiffness to high strength and stiffness, many different types of materials can be used as a honeycomb cores for sandwich structure. Metal and also nonmetal materials are used for its own purpose of use. Metallic honeycombs are resistant and less expensive, while nonmetallic honeycombs are not sensitive to corrosion and are good thermal insulators[17]. Honeycomb materials properties depend on the cell size and thickness of it. Thickness typically ranges from 3-50mm.

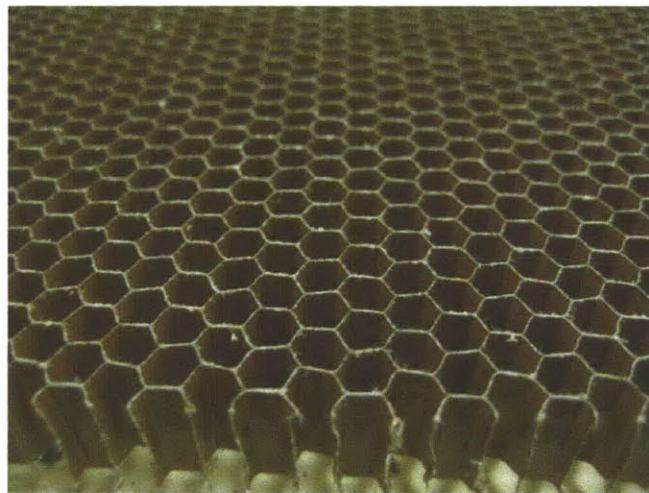


Figure 2.9 Honeycomb as a core material

2.2.2.1.2 Foam

Foams are possible materials for core sandwich structure for rotor blades because it's strong over compression force. Foams are manufactured by synthesizing polymers including polyvinyl chloride (PVC), polystyrene (PS), polyurethane (PU), polymethyl methacrylamide (acrylic), polyetherimide (PEI) and styreneacrylonitrile (SAN). It has density ranges of 30kg/m^3 to more than 300kg/m^3 , although the most used densities for composite structures range from 40 to 200 kg/m^3 [17].

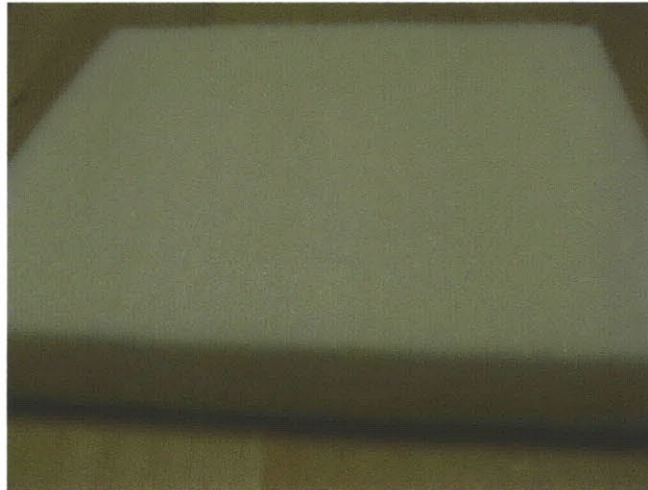


Figure 2.10 Light foam as a core material

2.2.2.1.3 Balsa

Woods can be described as 'nature's honeycomb', because it has a similar structure to the cellular hexagonal structure of synthetic honeycomb on a microscopic scale[17]. In order to play a similar role as a synthetic honeycomb structure the grain in

balsa wood should be arrayed to be perpendicular to the plane of the skins in a sandwich panel.

Balsa is the most commonly used wood core in a sandwich panel. Apart from its high compressive properties, it is a good thermal insulator offering good acoustic absorption. One of the disadvantages of balsa is that it has relatively high density among the core materials being used, with 100kg/m^3 . Its use is therefore normally restricted to projects where optimum weight saving is not required. Another disadvantage is that it will rot if it is not well surrounded by laminate or resin[17].



Figure 2.11 Balsa wood as a core material

2.2.2.2 Skin

For skin of sandwich structure high-strength composite facing sheets are used. Continuous fiber, woven, chopped fiber, hybrid composites are examples of composite skin. It is bonded to lightweight core materials by epoxy.

2.3 Designing and Manufacturing Samples

2.3.1 Sandwich Panels with Cork Core

Composite materials can be categorized into three broad categories depending on the type, geometry, and orientation of the reinforced fibers phase; particulate composites, discontinuous fibers composites, continuous fibers composites[15].

Inside the particulate composites, diverse sizes and shapes of particles are randomly scattered within the matrix. Because of this randomness of particle distribution, particulate composites are considered as quasi-homogeneous and quasi-isotropic in a macro scale.

Discontinuous fibers composites contain short fibers, which can be fairly long enough compared to their diameter, can be either all oriented along one direction or randomly oriented within matrix.

Continuous fibers composites are reinforced by long continuous fibers and are the most efficient form the point of view of stiffness and strength. Fibers can be all parallel, can be oriented at right angles to each other, or can be oriented along several directions.

Fiber reinforced composites also can be classified into broad categories according to the matrix used: polymer-, metal-, ceramic- and carbon matrix composites. For relatively low-temperature application such as composite materials for rotor blades polymer matrix are used primarily because of melting and softening at high temperature. There are two different types of polymer matrix: thermoset(epoxy, polyimide, polyester) and thermoplastic (Poly-ether-ether- ketone (PEEK), polysulfone). What matrix does in a composite structure is to bind the fibers together and keep the structure from external damage, transfers and distributes the applied loads to the fibers. A strong interface bond

between the fibers and matrix is desirable, so the matrix must be capable of developing a mechanical or chemical bond with the fibers. The fibers and matrix materials should be selected together in order to prevent chemically undesirable reaction at the interface.

In addition to the types discussed above, there are laminated composites consisting of thin layers of different materials bonded together.

The experiments in this study stray from using cork agglomerate and explore its form as filler additive to epoxy resin as a core materials in a sandwich panel. Glass fiber cloth (woven fabric with continuous fiber glass) is used for the out layer as a skin, and also the inclusion of chopped fiberglass strands with cork core is also explored to improve the mechanical properties. Since GRP are mainly used in manufacturing rotor blades of wind turbines, the control samples use fiberglass cloth and layers of fiberglass mat wetted through with epoxy resin.

2.3.1.1 Manufacturing Procedure

Cork composites and fiberglass samples are prepared in rough accordance with the ASTM D5687 procedure. Flat molds, two pieces of plywood covered by packaging tape, are used to make both samples. A layer of release fabric was placed on the bottom mold piece which is impermeable by tape, followed by lay-up, another layer of release fabric, breather material, the upper mold piece and more breather material to reduce sharp edges under the bag. Figure 2.12 shows the setup.

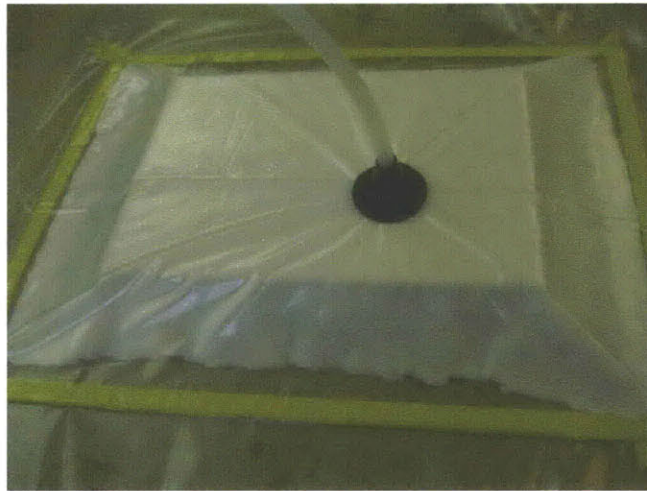


Figure 2.12 Vacuum bag setup

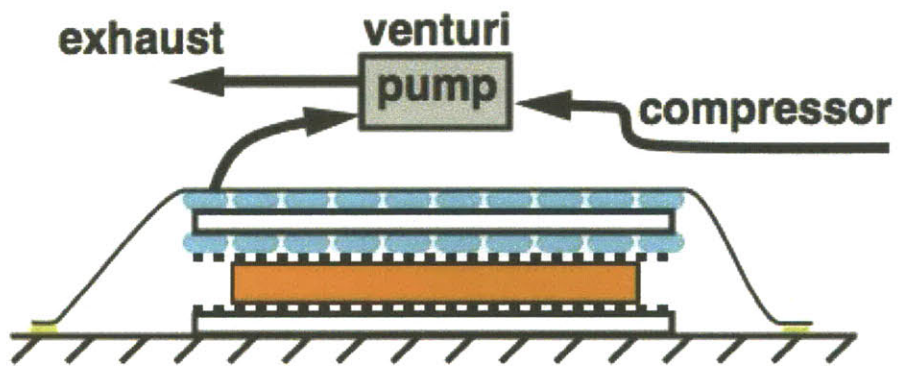


Figure 2.13 Cross section diagram of the vacuum bag setup [19]

Composites are cured under the evenly distributed pressure at 70psi for seven hours and should be remained without pressure for another seven hours for fully curing of the epoxy. Cork composites can be categorized into particulate composites with thermoset matrix (epoxy). Epoxy resin (West System #105 epoxy resin and #205 fast hardener) is chosen for matrix because of its superior chemical resistance, good adhesion, low cure shrinkage and high mechanical properties[14]. For making fiberglass samples in this study, woven mats are used as reinforcement.

2.3.1.2 Design Parameter Variation

2.3.1.2.1 Sizes of Cork Granules.

For this study, we have three different sizes of granulated cork: 1mm, 2-3mm, 4-5mm as shown in figure 2.14, 2.15, and 2.16. Cork composites using one size of cork granules have chasms and these chasms are usually filled with resin which results in making cork composites less dense. These chasms tend to be bigger when one bigger size of cork granules is mixed up with resin. Therefore, two different sizes of cork granules are mixed to lessen gaps between particulate. Three combinations of cork granules are obtained: Biggest + middle -, medium + finest-, Biggest + medium combinations. These three different combinations of cork composite are mixed with micro fibers to be tested in order to determine their improved property.



Figure 2.14 The biggest cork granules: 4-5mm



Figure 2.15 The medium size of cork granules: 2-3mm



Figure 2.16 The finest cork granules: 1mm

2.3.1.2.2 Amount of Epoxy

The fibers and the matrix are combined into the composite[1]. Many mixture combinations and mixing ratios can be incorporated and the composite properties of different combinations are mostly governed by the fibers, the matrix, and the way fibers are arranged into the composite. The important parameters are their relative amounts, often described by the fiber volume fraction[1].

Fiber volume fraction and matrix volume fraction are defined as

$$V_f = \frac{\text{Volume of fiber}}{\text{Total volume}} \quad (7)$$

$$V_m = \frac{\text{Volume of matrix}}{\text{Total volume}} \quad (8)$$

For example, the stiffness of the composite E_c is calculated according to

$$E_c = \eta \cdot V_f \cdot E_f + V_m \cdot E_m \quad (9)$$

Where,

E_c = the stiffness of the composite;

V = volume fraction; and

η = orientation factor (1/3 for randomly oriented fibers in two dimensions)

The strong correlation of volume fraction and stiffness of the composites can be seen from equation (9).

However, the fiber volume fractions are roughly determined by molding processes that can be used for making composites. Table shows common fiber volume fractions in different processes.

Molding Process	Fiber Volume Fraction
Contact Molding	30%
Compression Molding	40%
Filament Winding	60%~85%
Vacuum Molding	50%~80%

Table 2.1 Fiber volume fraction in different process [15]



Figure 2.17 Epoxy sneaked out through molds

For cork composites in this study, the optimum amounts of epoxy are determined by trials. If less epoxy is added to the cork combinations, the entire composites couldn't coat themselves well within amounts of epoxy added. Meanwhile adding too much epoxy in the composites makes left amount of epoxy that couldn't combine with cork smear out on outer breather which doesn't affect composites volume fraction actually. This happens because once amounts of cork granules in the composites are determined the ultimate gaps between cork granules can not be changed and are filled with some amounts of epoxy that needed to fill those chasms. Figure 2.18 shows the cork composites with not enough epoxy. In this study, the proper amount of epoxy in the composites is 20g per 3 g of fibers. The cork core composites consist of different sizes of cork granules and additional fillers mixed with epoxy resin at 1:2 ratio of cork to epoxy by volume.



Figure 2.18 A cork composite with less epoxy



Figure 2.19 A cork composite with resin at 1:2 ratio of cork to epoxy by volume

2.3.1.2.3 Additional Fiberglass Fillers

To lessen gaps in the composites and fortify their mechanical properties, two different types of fibers are added to pure cork granules making hybrid composites; micro fibers (West system #403 microfiber) and chopped glass stranded (James town). Their added amounts into the composites are restricted not to exceed the amounts of cork fibers because the main fibers in the composites are cork. The ratio of cork granules to fibers is fixed by 3:2 in this study.

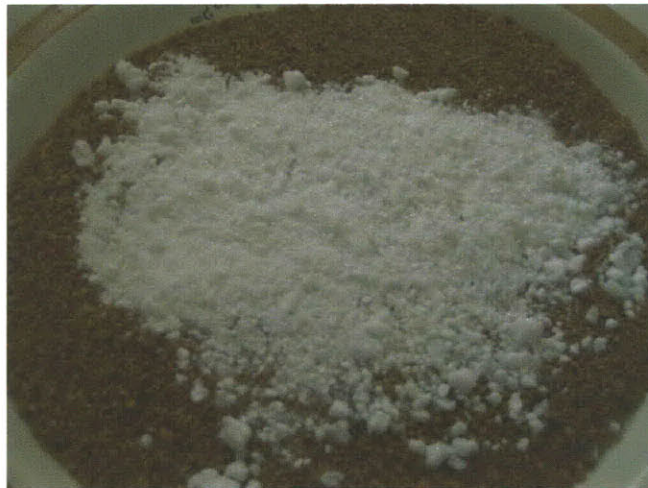


Figure 2.20 Cork granules with short fibers

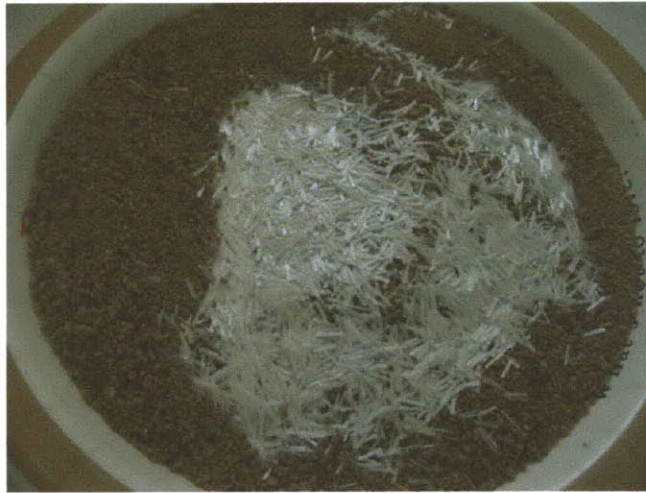


Figure 2.21 Cork granules with long fibers

2.3.1.2.4 Skin

Cork composites can be considered as a core material in this study. To determine the mechanical property cork composites as a core material for a sandwich panel, two different ways of adding skin onto cork composites was performed: one-sided- sandwich panels. One-sided panels have one skin at one side of cork composites and sandwich panels have two skins at both sides. The core cork composites are also tested without skin.

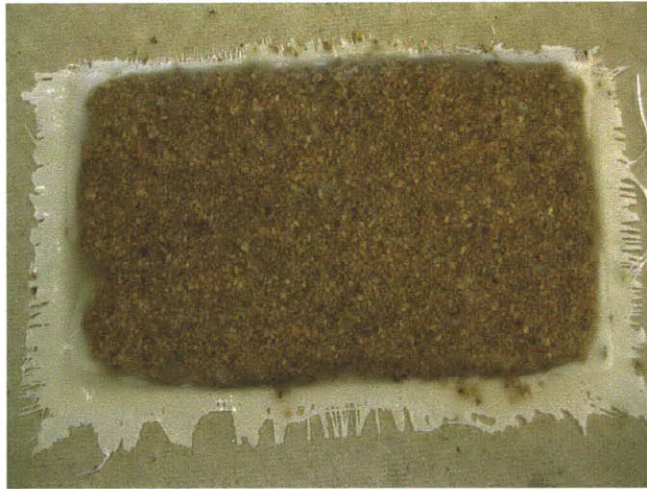


Figure 2.22 A one sided cork composite

2.3.2. Glass Reinforced Plastic (GRP)

Most rotor blades are made of GRP in the form of laminates. Therefore, we also made GRP as control samples for cork composites in order to compare their properties under the same condition.

GRP is one of composite materials made of a plastic reinforced by fine fibers made of glass. Polyester or vinylester, sometimes epoxy are often used as a matrix of composite materials. Many different types of fabric for GRP are manufactured and there are many different way to knit them[18]. When GRP woven or unidirectional fabrics are stacked up in a plastic matrix, a one layer of them is called a laminar and two or more then two is called a laminate[16]. A single glass fiber is strong with tension and compression along its axis while it is not with shear. By laying them with different orientation of each layered up fabrics, its strength can be fortified[18].

2.3.2.1 Manufacturing Procedure

The control samples consist of two layers of fiberglass cloth and ten layers of chopped strand fiberglass mats (0.75 oz/ft²), wet through with West System #105 epoxy resin and #205 fast hardener. Mats are fabrics made of short fibers (length between 5 and 10 cm). It is isotropic within their plane because short fibers are randomly oriented. After cutting fiberglass mats and cloths into the size for flat molds, every layer should be wetted through matrix (epoxy with hardener) by hands. Using same vacuum bagging setup that used for making cork composite, fiberglass samples should be placed between two flat molds during 7 hours under the pressure at 70 psi. After curing 7 hours in the vacuum bag setup, it should be left sitting alone another 7 hours to be perfectly cured.



Figure 2.23 Randomly Oriented fiberglass mat

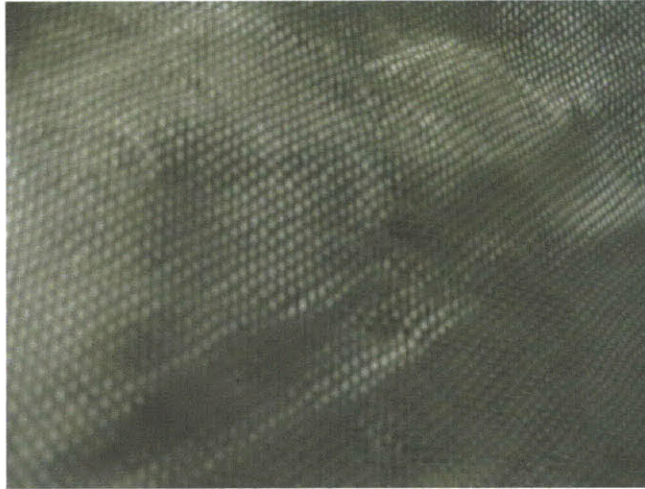


Figure 2.24 Fiberglass cloth for a skin



Figure 2.25 Ten layers of fiberglass mats wetted through epoxy on the bottom mold

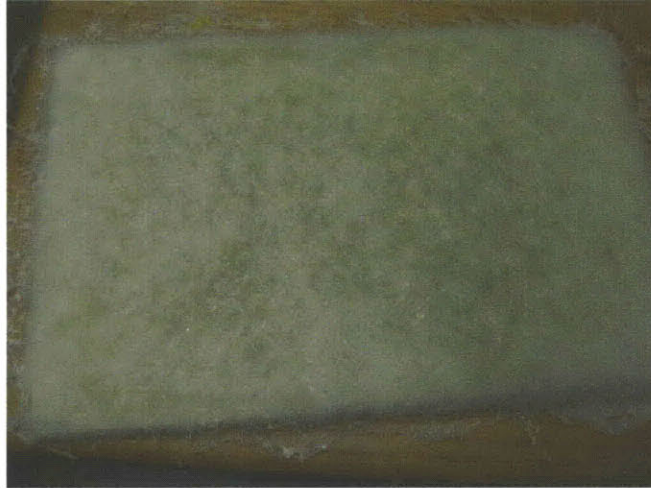


Figure 2.26 Fiberglass sample



Figure 2.27 A fiberglass specimen for bending test

2.3.2.2 Design Parameter Variations

In order to have different GRP structures as control samples for cork composites, two different types of fiberglass samples are made: sandwich panels with two skins and ten layers of mats between them and one sided samples that has a skin at one side after stacking ten layers of mats. The amounts of epoxy used to wet fibers are roughly fixed because there are certain portions of porous parts inside the mats. The amounts that make 10 mats of fibers fully saturated are considered as used epoxy amounts: one pump (20g of epoxy) for one layer.

2.4 Evaluation of Properties

2.4.1 Strength

2.4.1.1 Bending Test

2.4.1.1.1 Background Theory

The flexure equation for a composite beam incorporates the modulus of elasticity of the material being examined E , the moment M exerted on the beam, the distance y from the neutral axis, and an effective flexural stiffness, $(EI)_{eff}$,

$$\sigma = \frac{EMy}{(EI)_{eff}} \quad (10)$$

Where

I = the area moment of inertia.

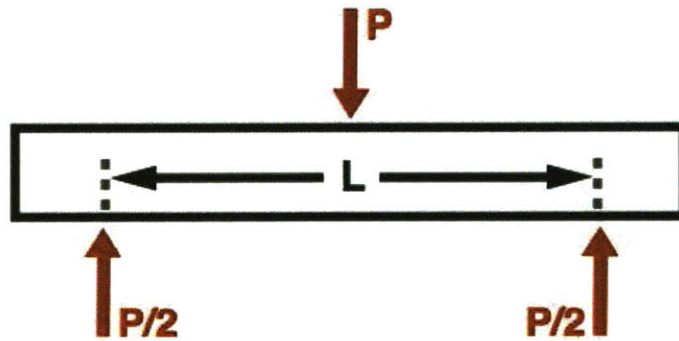


Figure 2.28 A beam undergoing a three-point bending load [19]

During a three-point bending load applying, the moment varies along the span, the x -axis, according to

$$M(x) = \frac{P}{2} \left(\frac{L}{2} - x \right), \quad (11)$$

Where

$x = 0$ at the center of the beam;

P = the load;

L = the length of the support span.

The moment is the greatest at the center of the span. Load and displacement can be related to the flexural stiffness by using the moment-curvature relation for small deflections, u :

$$M = \frac{(EI)_{eff}}{\rho} \approx (EI)_{eff} \frac{\partial^2 u}{\partial x^2}, \quad (12)$$

Where

ρ = the radius of curvature of the beam.

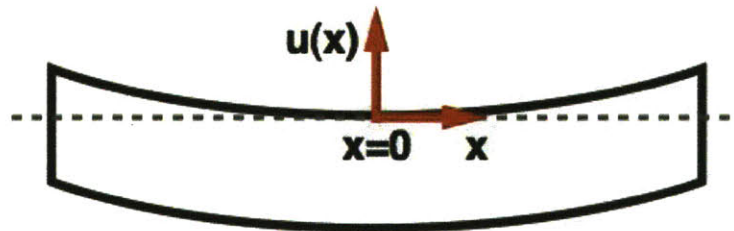


Figure 2.29 Display of coordinate system on a beam [19]

After plugging equation (10) into equation (11) and integrating equation (12) twice, then equation (13) is obtained.

$$(EI)_{eff} = \frac{PL^3}{48u} \quad (13)$$

The area of moment inertia of beam can be expressed as

$$I = \frac{bh^3}{12}, \quad (14)$$

Where

b = the width of the beam tested, and

h = the thickness.

The experiments data recorded only have applying loads to specimen and displacements of specimen correspondingly. For the composites in this study, the specimens are deflected until rupture occurs either in the outer surface of the test specimen or on entire specimen. The Flexural stress from the test can be calculated by the equation from ASTM D790. The flexural strength is the maximum flexural stress during the bending test.

$$\sigma_f = 3PL / 2bh^2 \quad (15)$$

Where

σ_f = stress in the outer fibers at midpoint,

P = load at a given point on the load-deflection curve,

L = the length of the support span,

b = the width of beam tested, and

h = the thickness.

The flexural strain indicates that changes in the length of an element of the outer surface of the test specimen at midspan by flexural stress. The flexural strain is also calculated by using equation (16).

$$\varepsilon_f = 6Dh/L^2 \quad (16)$$

Where

ε_f = strain in the outer surface,

D = maximum deflection of the center of the beam,

L = the length of the support span, and

h = thickness.

The flexural modulus of elasticity, often called the “modulus of elasticity,” is the ratio of stress to corresponding strain within the elastic limit. It is calculated by following equation.

$$E_b = \frac{L^3 m}{4bd^3} \quad (17)$$

Where

E_b = modulus of elasticity in bending,

L = the length of the support span,

b = the width of beam tested,

h = the thickness, and

m = slope of the tangent to the initial straight-line portion of the load-deflection curve.

Since the above equations are used to calculate the properties from experimental data, they can be applied to both of cork core composites and sandwich panels. However,

theoretical calculations for composite properties from the book are also possible and worthy to compare to experimental calculation.

For composites

$$V_f = \frac{\text{Volume of fiber}}{\text{Total volume}} \qquad V_m = \frac{\text{Volume of matrix}}{\text{Total volume}}$$

The stiffness of the composite E_c is calculated according to

	$E_c = \eta \cdot V_f \cdot E_f + V_m \cdot E_m$	(18)
--	--	------

Where,

E_c = the stiffness of the composite

V = volume fraction

η = orientation factor (1/3 for randomly oriented fibers in two dimensions) [1]

For sandwich structure

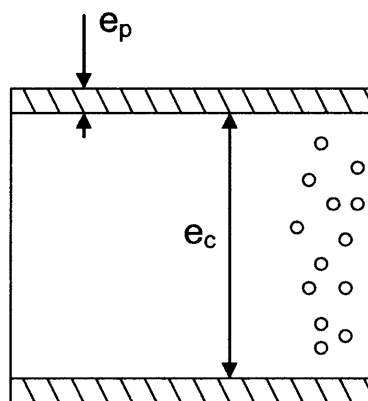


Figure 2.30 A sandwich structure cross section: e_p and e_c indicate the thickness of skin and core respectively

$$(EI)_{eff} = E_p e_p \frac{(e_p + e_c)^2}{2} \quad (19)$$

Where,

e_p = the thickness of skin,

e_c = the thickness of core, and

E_p = the modulus of elasticity of the material of skin [16]

2.4.1.1.2 Experimental Setup

Testing protocol was based off of the ASTM D790 procedure, which covers the determination of flexural properties of unreinforced and reinforced plastics.

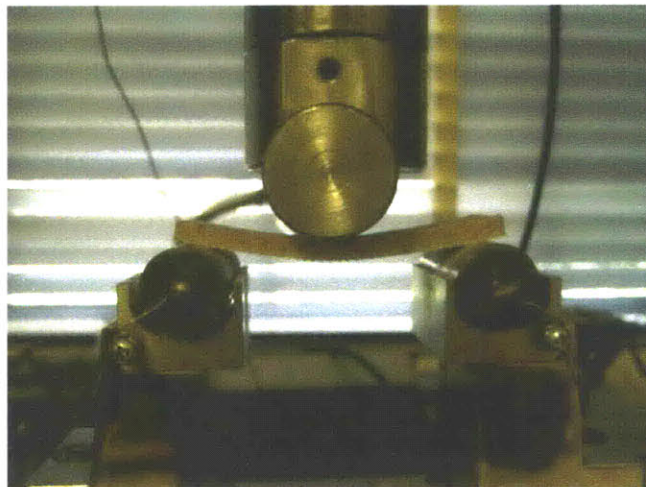


Figure 2.31 Bending test setup

Apparatus

The Instron 1125, modified by ADMET to include load control, is the test machine with a 20kN loading cell. The appropriate strain rate is calculated according to ASTM D790.

$$R = ZL^3 / 6h \quad (20)$$

Where,

R = rate of crosshead motion, i.e. strain rate,

L = support span,

h = the thickness of beam tested, and

Z = rate of straining of the outer fiber, mm/mm/min. Z shall be equal to 0.01.

The strain rate is changed for each sample group after measuring the thickness of each samples and averaging them. The support span is 90mm for the specimens that have a span-to-thickness ratio greater than 16:1. The radii of the supports are 12.7 mm and that of the loading nose was 19 mm, differing from the 5mm radii called for by the protocol. Each sample group should be tested with at least 5 specimens.

Specimens

The specimens are machined down to the length of 100mm, and width of 25mm. Even the thickness of the specimens differs from not only each sample group and also each specimen in the same group, they are relatively thin compared to their length, less than 1/16 times of their length.



Figure 2.32 A sandwiched cork specimen for bending test

2.4.1.1.3 Results and Analysis

For cork core composites, three different sizes of cork granules are compounded making three different combinations: Biggest + middle -, middle + finest-, Biggest + middle combinations. These three different groups of cork composites are tested first in order to find which combination is the strongest one.

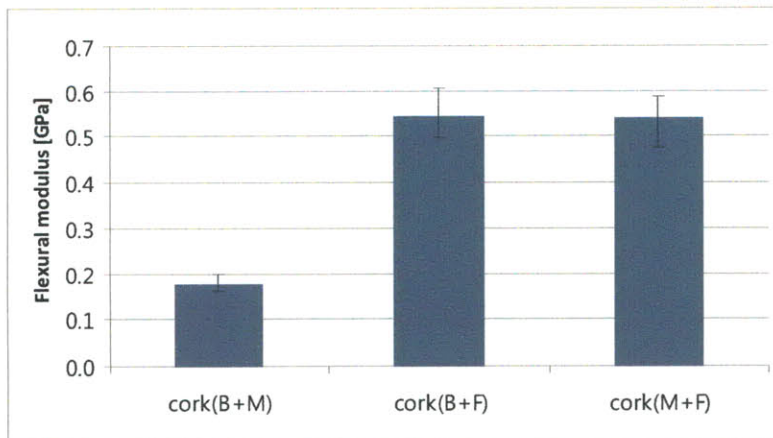


Figure 2.33 Flexural modulus of pure cork composites

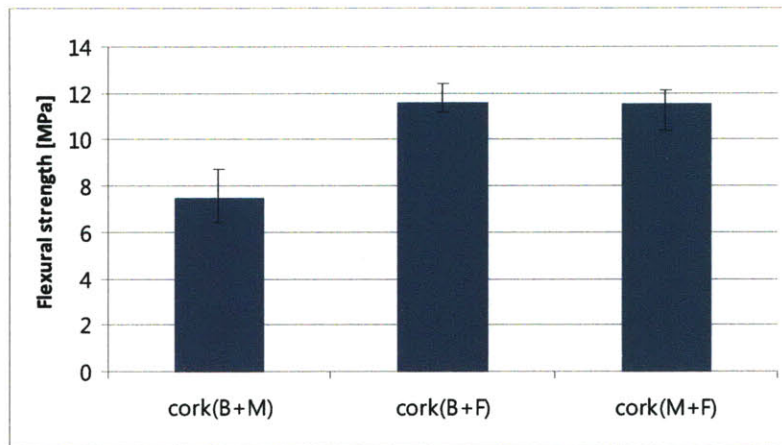


Figure 2.34 Flexural strength of pure cork composites

	Cork(B+M)	Cork(B+F)	Cork(M+F)
Density [Mg/ m^6]	0.58	0.58	0.58
Flexural Modulus [GPa]	0.17	0.54	0.54
Flexural strength [MPa]	7.52	11.58	11.53

Table 2.2 The results of bending test showing the strongest cork combination

To improve its mechanical properties by lessening the gaps between cork granules chopped fiberglass strands, which are named long fibers in this study, and micro fibers, which are also named short fibers in this study, are added to the pure cork granules.

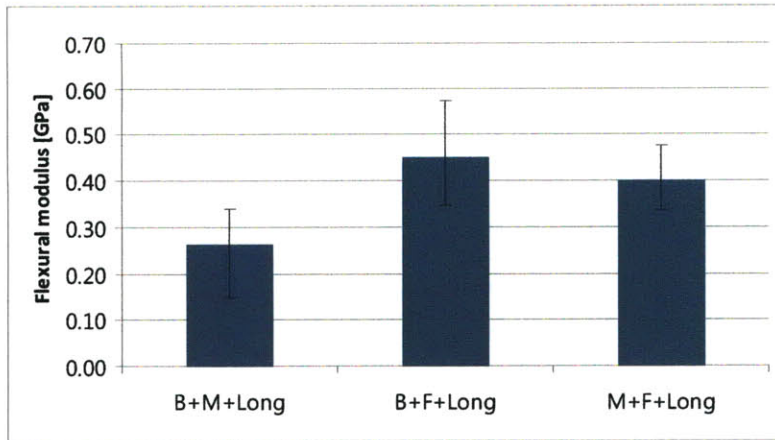


Figure 2.35 Flexural modulus of cork composites with long fibers

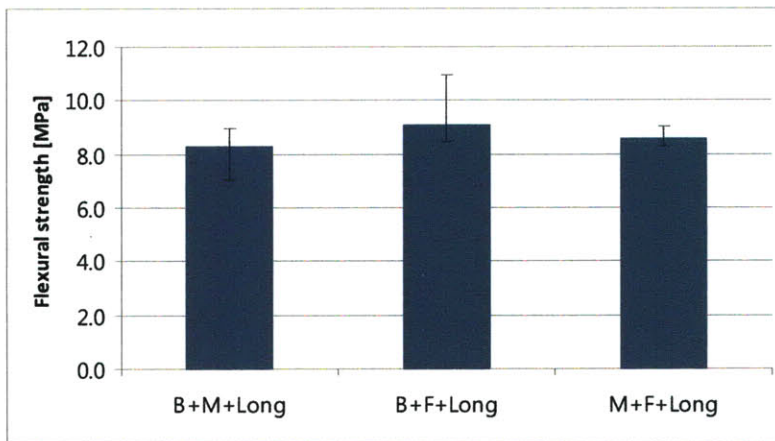


Figure 2.36 Flexural strength of cork composites with long fibers

	Cork(B+M+Long)	Cork(B+F+Long)	Cork(M+F+Long)
Density [Mg/ m ³]	0.62	0.62	0.62
Flexural Modulus [GPa]	0.26	0.45	0.4
Flexural strength [MPa]	8.31	9.12	8.62

Table 2.3 The results of bending test showing the strongest cork combination with long fibers

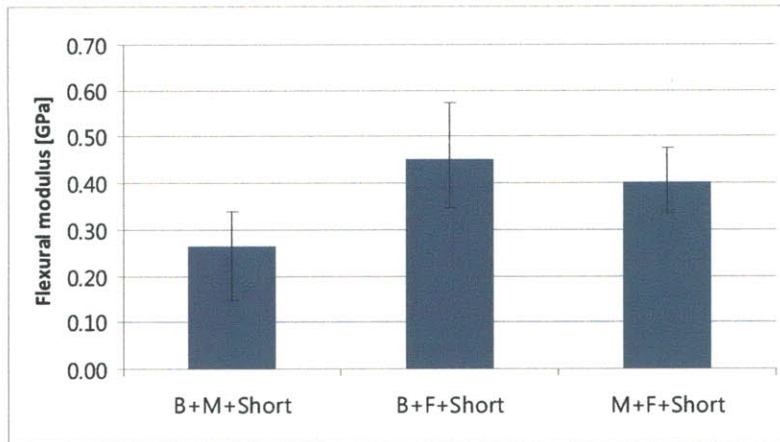


Figure 2.37 Flexural modulus of cork composites with short fibers

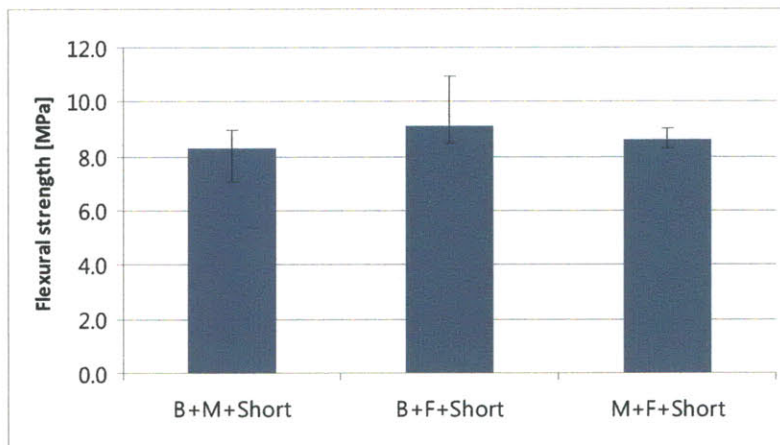


Figure 2.38 Flexural strength of cork composites with short fibers

	Cork(B+M+Short)	Cork(B+F+Short)	Cork(M+F+Short)
Density [Mg/ m ³]	0.67	0.67	0.67
Flexural Modulus [GPa]	0.90	0.93	0.85
Flexural strength [MPa]	12.62	15.02	10.07

Table 2.4 The results of bending test showing the strongest cork combination with short fibers

For cork core composites, the strongest combination is obtained: Biggest+ finest+ short fiber. Before the test cork core with longer fibers were expected to have higher strength than short fibers in the cork core composites making the bond between cork granules and itself stronger within a matrix. However the result is different what we expected. The reason is that short fibers lesson the gaps between fillers effectively than longer fibers making entire stiffness of material stronger against the stress.



Figure 2.39 Core cork with short fibers and epoxy

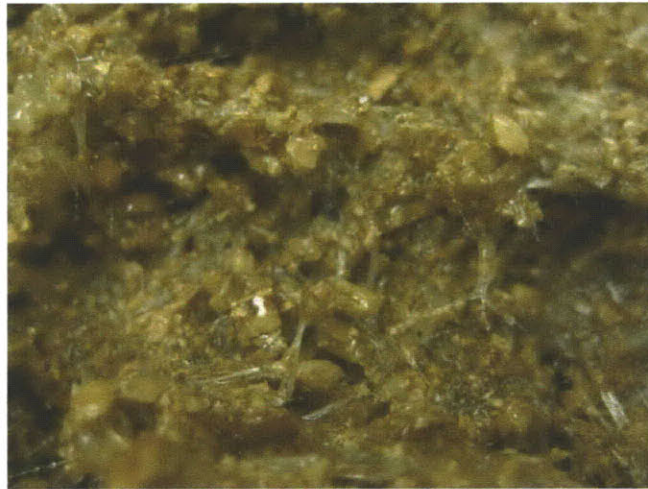


Figure 2.40 Core cork with long fibers and epoxy

By covering one or both sides of the strongest combination of cork composites with fiberglass cloth, one-sided cork composites and sandwiched cork composites are obtained. The results are compared to those of fiberglass specimens that consist of 10 layers of mats with skin on one or both sides.

	One sided cork composites	Sandwiched cork composites	One sided Fiberglass	Sandwiched Fiberglass
Density [Mg/ m ³]	0.69	0.73	1.32	1.36
Flexural Modulus [GPa]	1.16	4.69	8.17	8.92
Flexural strength [MPa]	40.71	48.69	201.82	207.95

Table 2.5 The results of bending test

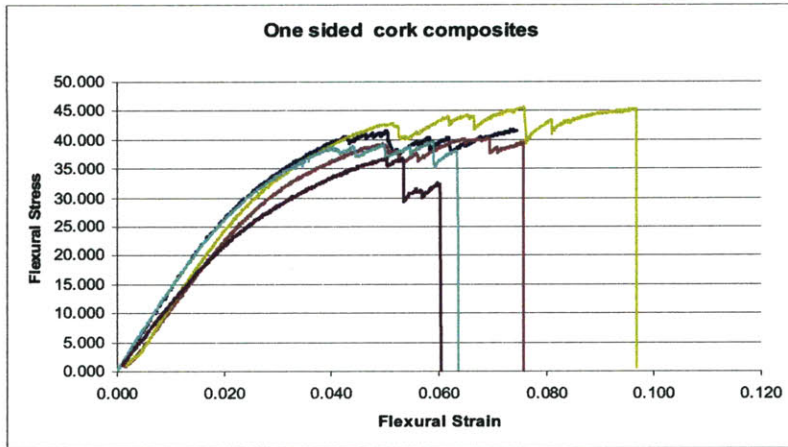


Figure 2.41 The graph of one sided cork composite from bending test

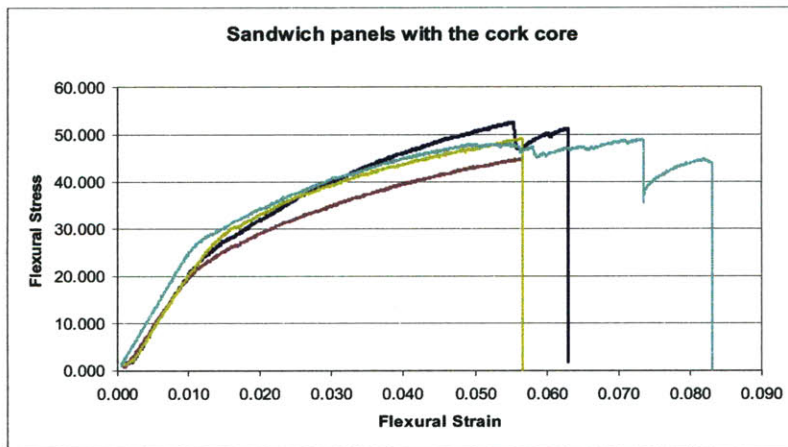


Figure 2.42 The graph of sandwiched cork composites from bending test

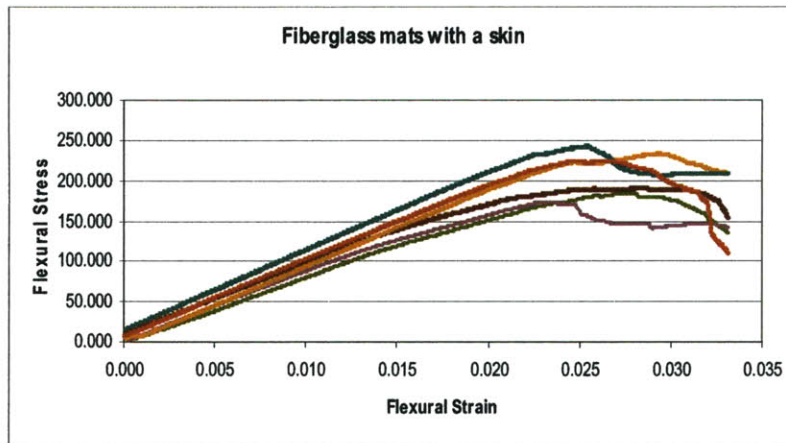


Figure 2.43 The graph one sided fiberglass samples from bending test

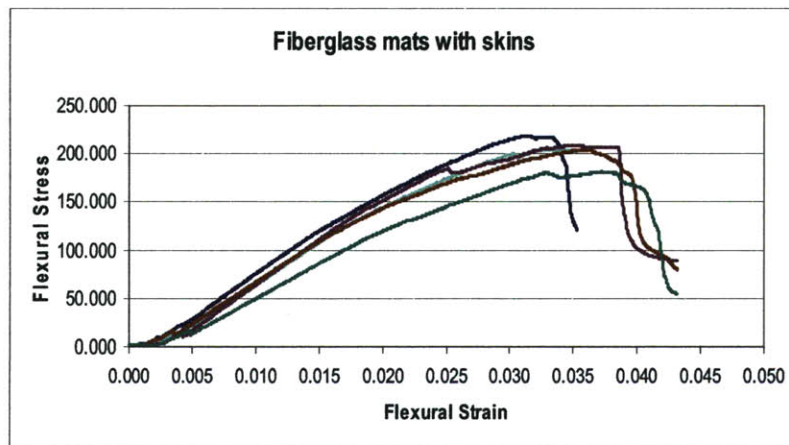


Figure 2.44 The graph of sandwiched fiberglass samples from bending test

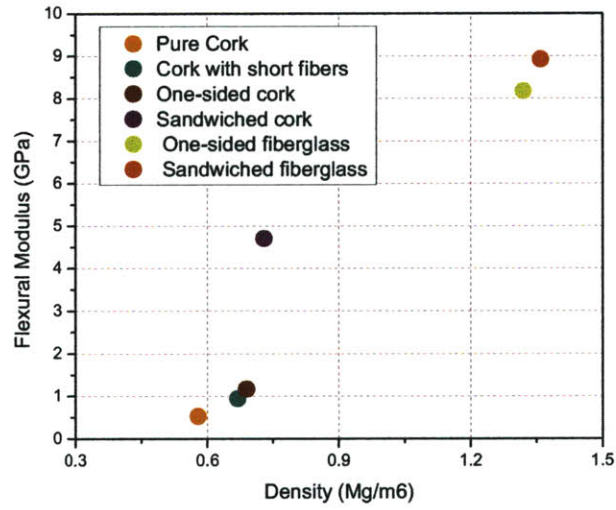


Figure 2.45 The density versus flexural modulus for tested samples

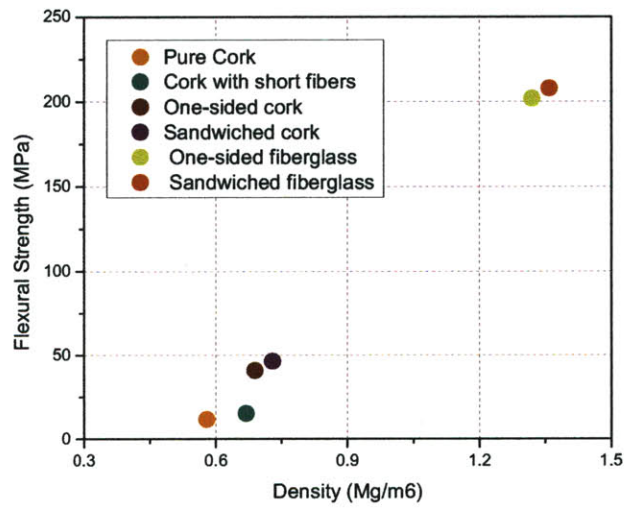


Figure 2.46 The density versus flexural strength for tested samples

Figure 2.45 and 2.46 schematically show the density versus flexural modulus and strength of all tested samples on the same figure.

To summarize the tests results, the strongest cork core composites is the mixture with the biggest and the finest and short fibers. Among pure cork core, mixture of the biggest and the finest cork granules has the highest modulus and strength. The finest cork effectively fills the porous gaps. In the same sense, short fibers are strongly bonded to cork granules with epoxy diminishing the chasm effectively. Longer fibers usually added other composites to improve their total strength and modulus. However, in this research this doesn't affect their strength and modulus compared to short fiber. That is because the main filler, cork granules, in this composite is not generally used materials in composites such other fiberglass fabric which will be strongly combined with longer fibers. A sandwiched cork composite with short fibers is the strongest structure. It has almost half of the fiberglass density and a quarter of flexural modulus and strength. The results can not meet the requirements that the modulus should range from 10 to 20 GPa in order to become a rotor blade material. However, as seen from figure 2.47, the fiberglass composites and cork composites lie on the same line which means they have the same nominal modulus versus density. Also, the modulus of cork composites surpasses the modulus of wood. Just in terms of modulus comparison, after delicate manufacturing sandwiched cork composite, it could substitute the rotor blade made of wood.

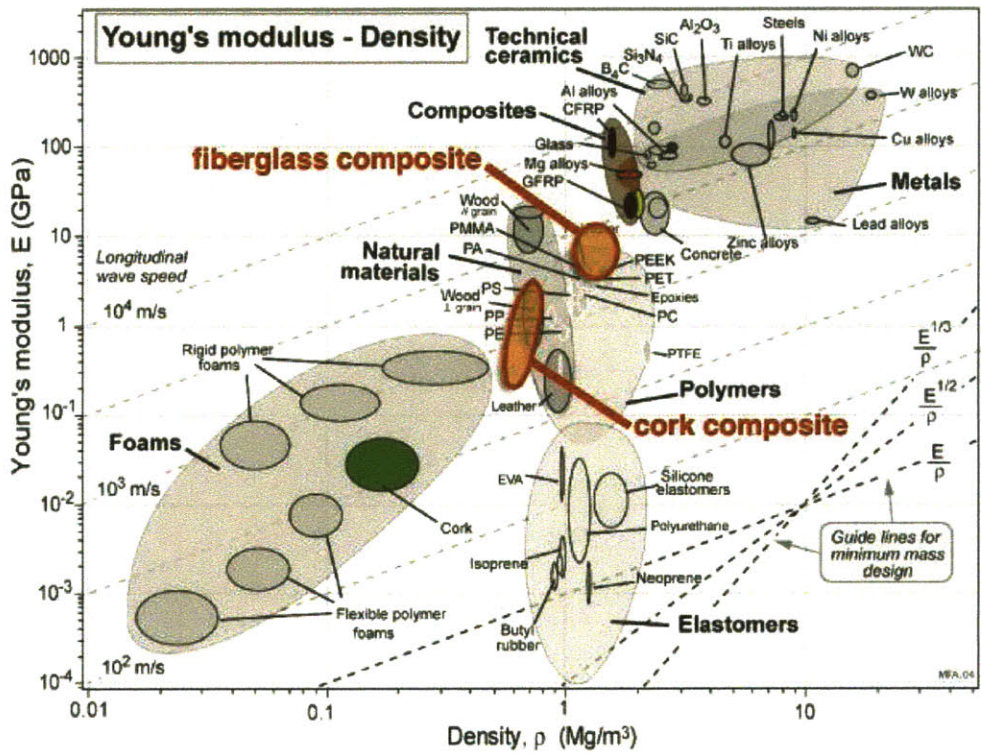


Figure 2.47 Ashby chart showing where the flexural modulus of samples are located

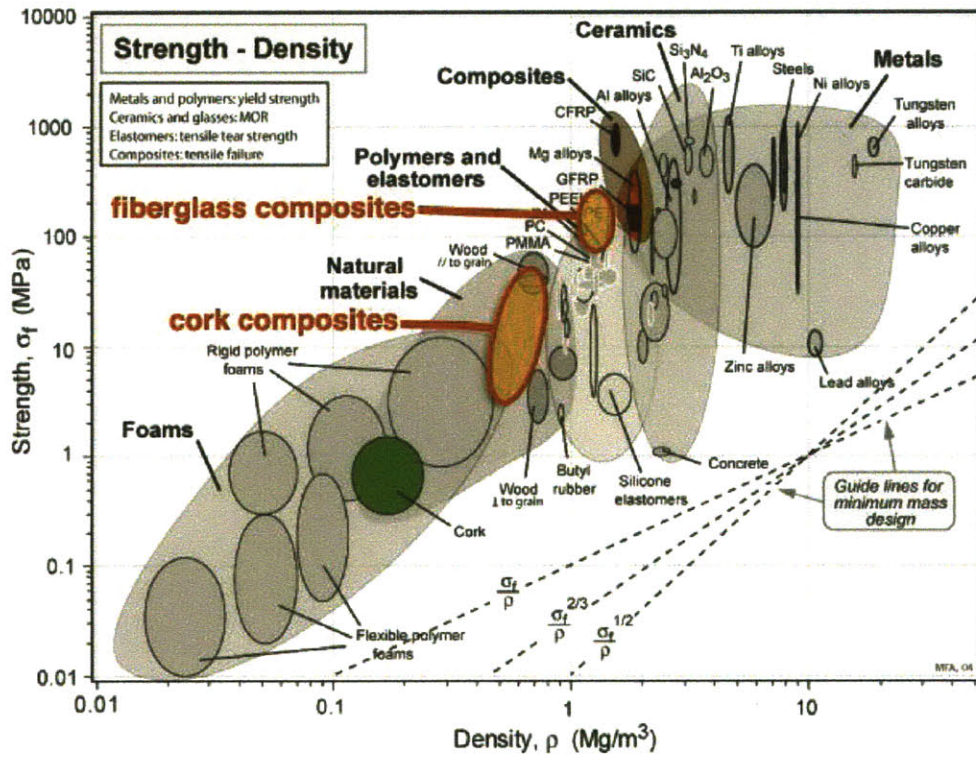


Figure 2.48 Ashby chart showing where the flexural strength of samples are located

2.4.1.2. Tensile Test

2.4.1.2.1 Background theory

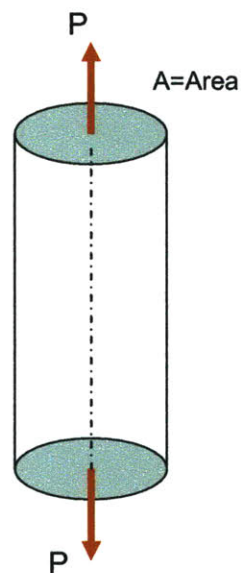


Figure 2.49 Bar carrying normal, tensile load P

The end of bar carrying normal load of P gives the stress σ over the cross section A. If the length of bar is longer than 2.5 times of bar's diameter, than the stress over the cross section can be assumed that it is evenly distributed.

$$\sigma = \frac{P}{A} \quad (21)$$

Where

P = normal load to the surface

A = area of the cross section

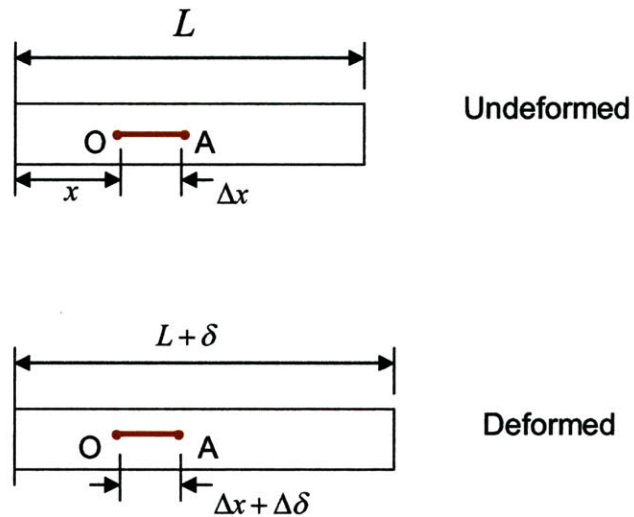


Figure 2.50 Elongation of the bar caused by force

When the elongation δ caused by an applied force is divided by the overall length L , it can be defined as the elongation per unit length, i.e. strain ε .

$$\varepsilon = \frac{\delta}{L} \quad (22)$$

Where

L = length of the bar, and

δ = elongation of the bar when a force applied.

Stress is proportional to strain

$$\sigma = E\varepsilon \quad (23)$$

Where,

E= Elastic modulus

If we assume that the stress caused by P is below the proportional limit, then the equation (21) is applicable to calculate the elongation. After plugging equation (21) and (22) into equation (23), the equation (24) for elongation of bar is obtained.

$$\sigma = \frac{\sigma L}{E} = \frac{PL}{EA} \quad (24)$$

2.4.1.2.2 Experimental Setup

Testing protocol was based off of the ASTM D638 procedure, which covers the determination of tensile properties of plastics.

Apparatus

For the tensile test, the Instron 5582 is used with a strain rate calculated according to ASTM 638. For the specimen whose thickness is less than 7 mm should be 5 mm/min.

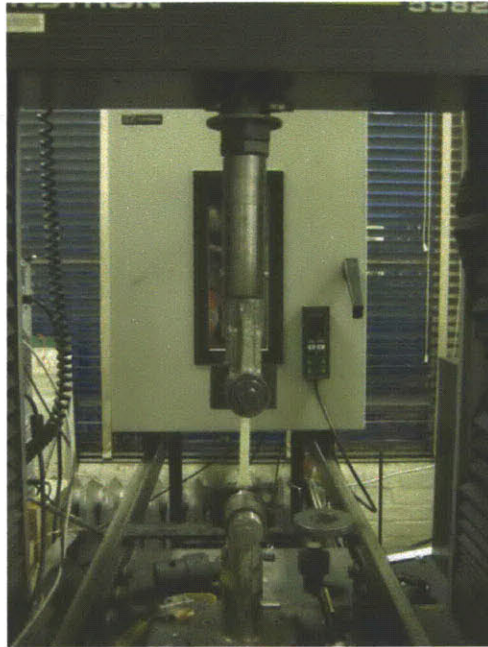


Figure 2.51 Tensile test setup

Specimens

For tensile test, there are several types of specimen shapes according to the thickness of the sample. Our composites have less than 7mm thickness. Figure 2.52 and 2.53 show the specimen for tensile test based on ASTM 6380.

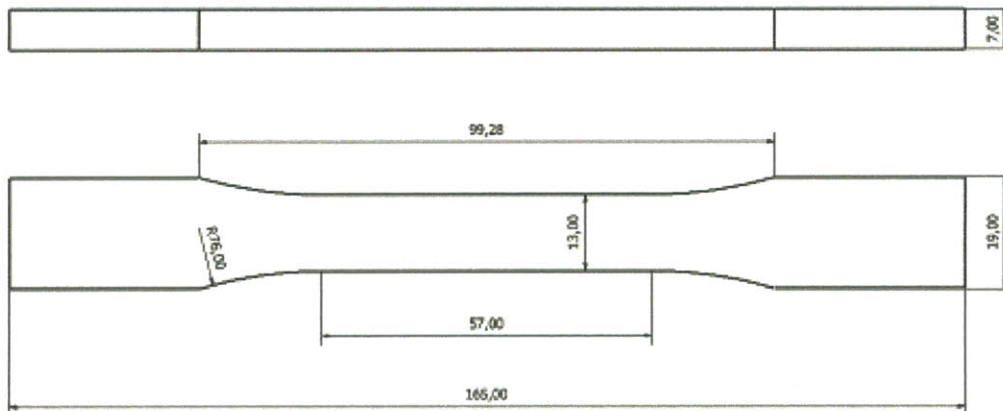


Figure 2.52 Dimension of specimen for tensile test

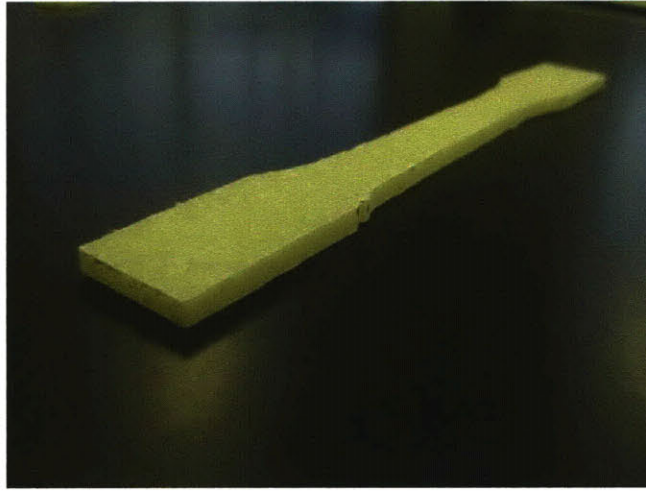


Figure 2.53 A tensile specimen

2.4.1.2.3 Results and Analysis

Three different pure cork composite combinations are tested in order to find the strongest combination by tensile test as well.

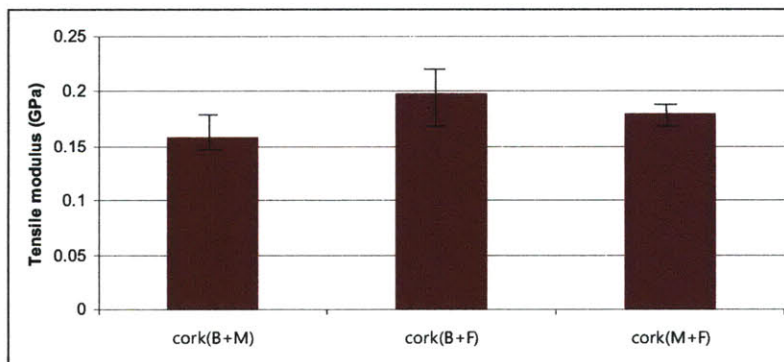


Figure 2.54 Tensile modulus of pure cork composites

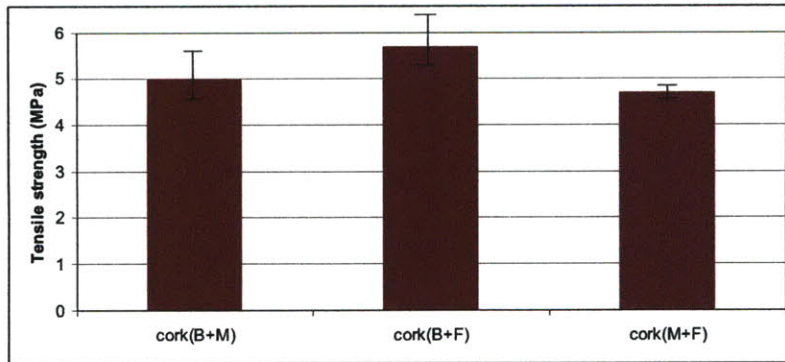


Figure 2.55 Tensile strength of pure cork composites

	Cork(B+M)	Cork(B+F)	Cork(M+F)
Density [Mg/ m^6]	0.58	0.58	0.58
Tensile modulus [GPa]	0.16	0.19	0.18
Tensile strength [MPa]	4.98	5.69	4.69

Table 2.6 The results of tensile test showing the strongest cork combination

The results from the tensile test on pure cork composites show the same tendency about which combination is the strongest even though the modulus and strength is not as high as those from flexural tests. It is needed to check the effect of additional fillers on modulus and strength of the strongest pure cork composite combinations.

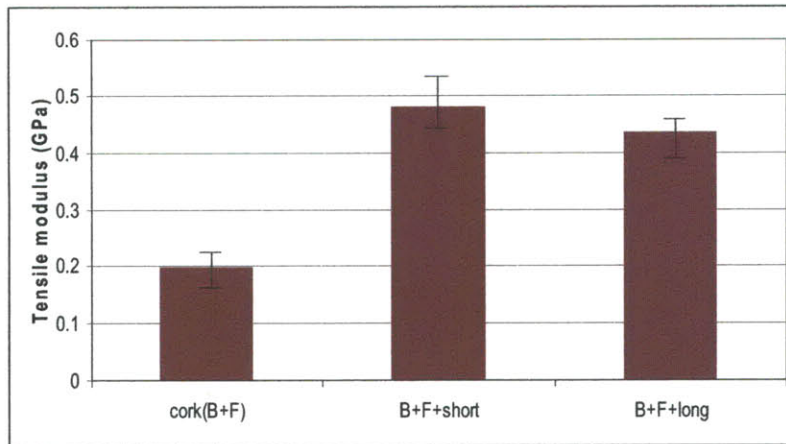


Figure 2.56 Tensile modulus of cork composites with(short, long)/without fibers

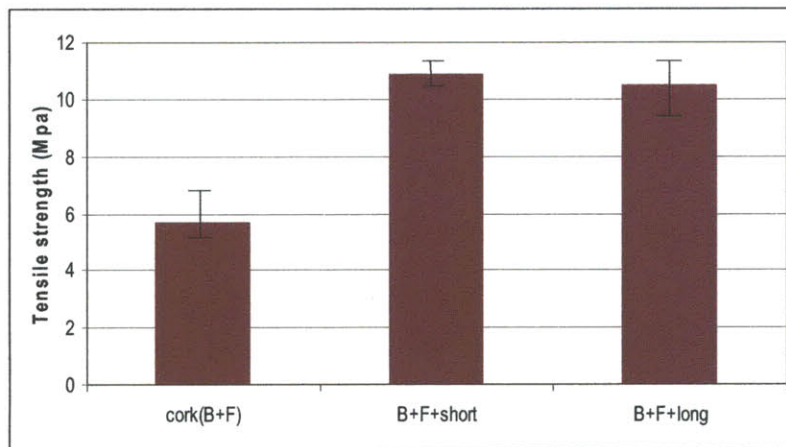


Figure 2.57 Tensile strength of cork composites with(short, long)/without fibers

	Cork(B+F)	B+F+short	B+F+long
Density [Mg/ m ⁶]	0.58	0.67	0.62
Tensile modulus [GPa]	0.19	0.48	0.44
Tensile strength [MPa]	5.69	10.9	10.5

Table 2.7 The results of tensile test showing the strongest cork combination

The results of tensile modulus and tensile strength for both cork composites with short/ long fibers show that there is no big difference between the use of short/ long fibers on tensile modulus as well as strength. However, unlike the results from bending test, the both values on modulus and strength for cork core composites with long fibers is almost same as composites with short fibers.

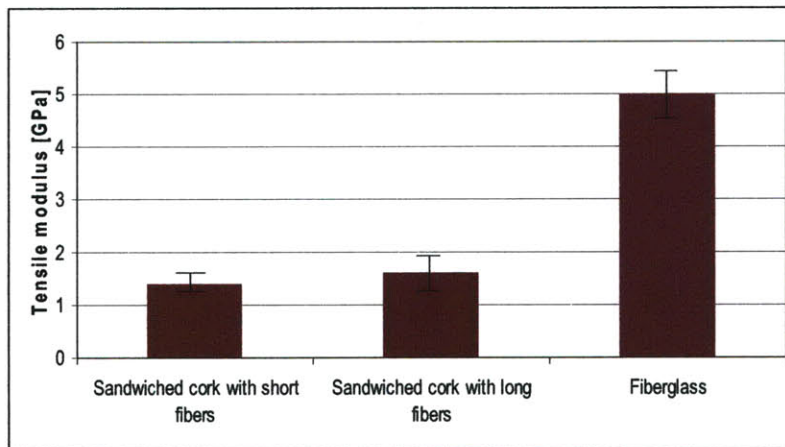


Figure 2.58 Tensile modulus of fiberglass and cork composites with skin and fibers

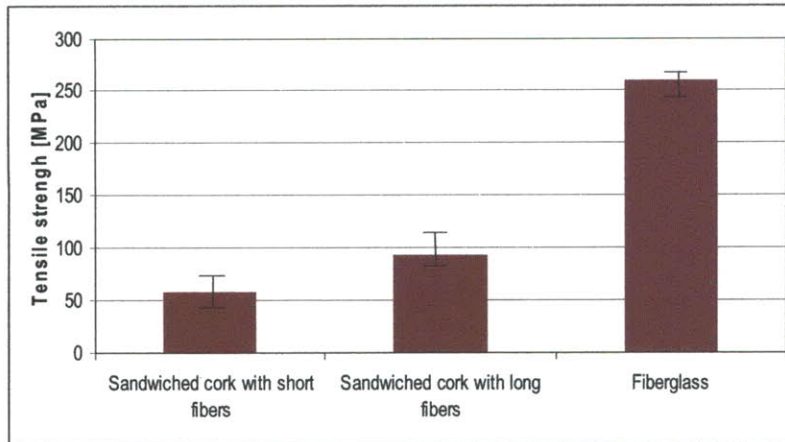


Figure 2.59 Tensile strength of fiberglass and cork composites with skin and fibers

	Sandwiched cork with short fibers	Sandwiched cork with long fibers	Fiberglass
Density [Mg/m^3]	0.73	0.71	1.36
Tensile modulus [GPa]	1.38	1.62	5.01
Tensile strength [MPa]	57.38	92.2	259.79

Table 2.8 The results of tensile test

When skins are attached to both sides making sandwiched cork, the results shows the different aspects from the bending test: the tensile modulus of sandwiched cork with short fibers is less than flexural modulus but the tensile strength is bigger than flexural strength. One more interesting to look at is the tensile results of sandwiched cork with long fibers. From bending test results, long fibers don't play an important role to fortify

the mechanical properties by adding them into pure cork core. However, for tensile test, the results show that both modulus and strength with long fibers are almost as strong as with short fibers. Due to the fact that long fibers don't help gaps between cork lessen effectively this results should be reasoned.

Figure 2.60 and 2.61 schematically show the density versus tensile modulus and strength of all tested samples on the same figure.

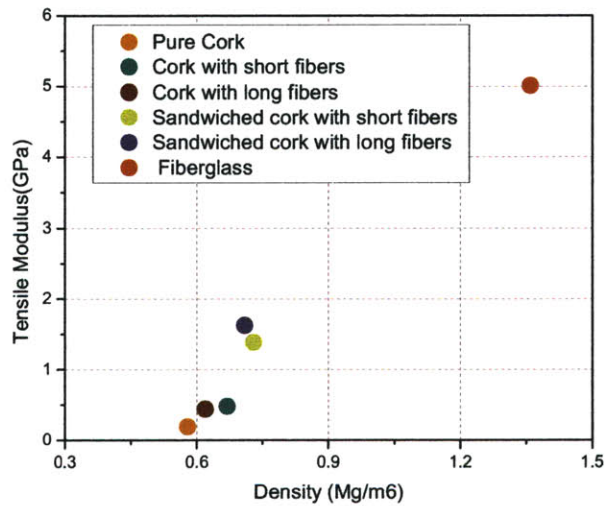


Figure 2.60 The density versus tensile modulus for tested samples

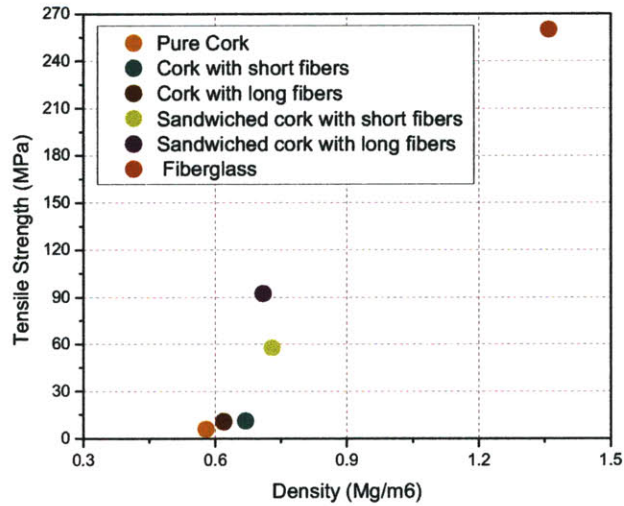


Figure 2.61 The density versus tensile strength for tested samples

The tensile and flexural properties can be compared to each other to where the properties can be placed on the density- properties charts. As we already expected, the results are quite matched to each other. The modulus from tensile and bending tests can be also compared with the results from the dynamic mechanical analysis results. However, it turned out that results are quite different in this study with results from the dynamic mechanical analysis results, because the applied force for dynamic mechanical analysis is a sinusoidal with changing frequency.

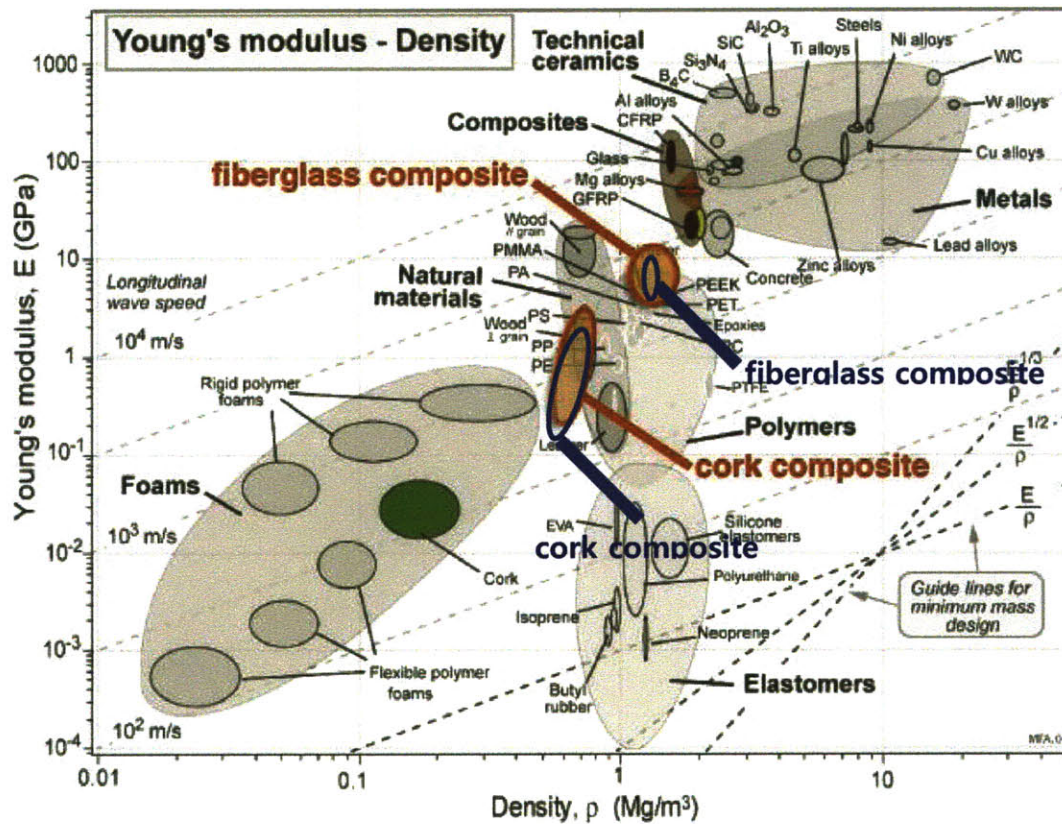


Figure 2.62 Ashby chart showing where the flexural and tensile modulus of samples are located

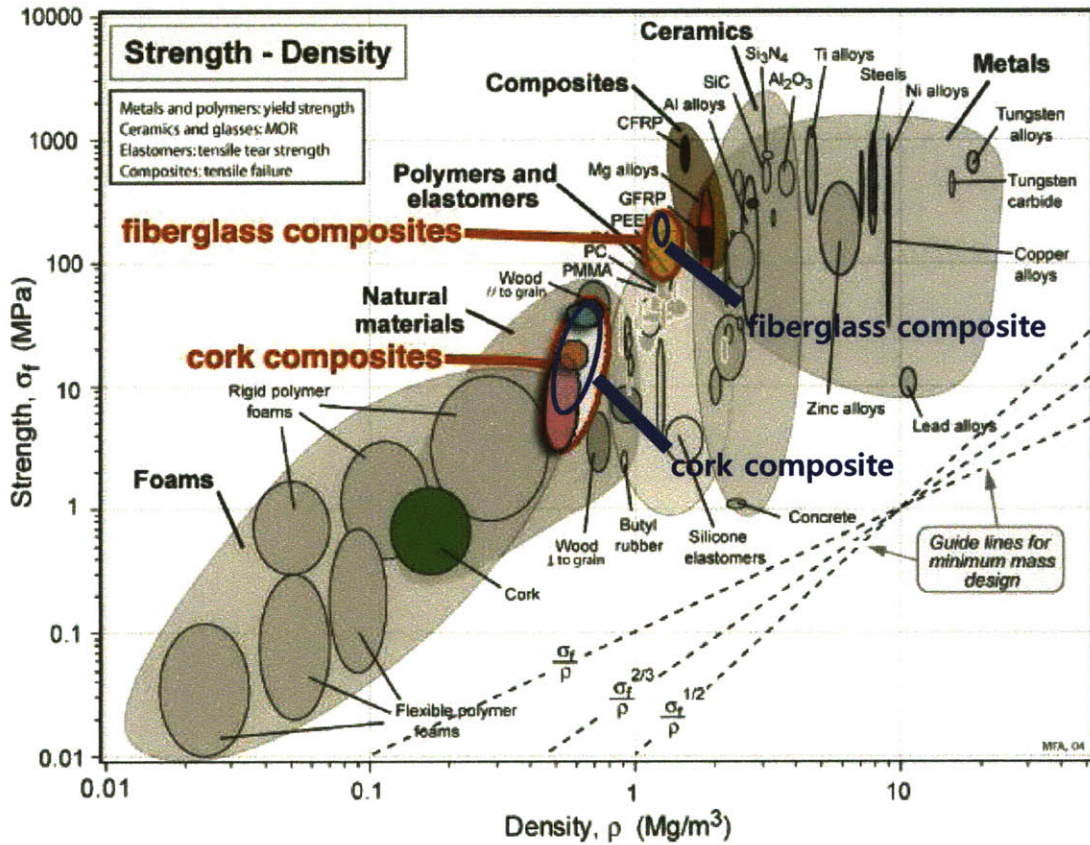


Figure 2.63 Ashby chart showing where the flexural and tensile strength of samples are located

2.4.1.3 Charpy V-notch Test

2.4.1.3.1 Background Theory

In order to determine the resistance of composite materials, a Charpy V-notch test, also known as Charpy impact test, is conducted. The testing protocol was based off of the ASTM D6110 procedure, which covers the determination of Charpy Impact Resistance of Notched Specimens of Plastics. Calculating the impact resistance of the materials to breakage by flexural shock is executed by testing apparatus that consists of a simple pendulum [20],[21]. The apparatus measures the angle θ at which the specimen is broken by one single pendulum swing. The results of this test method are reported in terms of energy absorbed per unit of specimen width. However in this study, due to the variance of specimen's thickness, the resistance over the area is calculated.

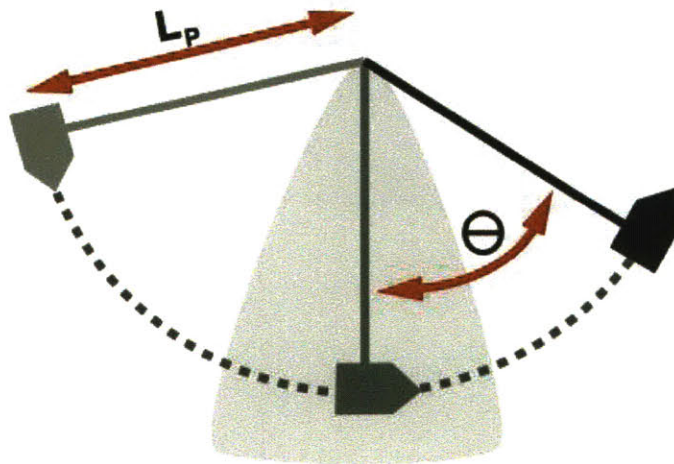


Figure 2.64 Dimensions of Charpy testing apparatus [19]

First, the machine is run without a sample to calibrate the results to a maximum value, E_{max} .

To convert from the angle reading θ to energy, the following formula is used:

$$E_{raw} = L_p W_p (1 - \cos \theta) \quad (25)$$

Where

L_p = the length of the pendulum arm, and

W_p = the weight of the pendulum head.

The energy required to break the specimens, E_{CVN} , is calculated by subtracting E_{raw} from E_{max} , thus eliminating the effects of friction and windage:

$$E_{CVN} = E_{max} - E_{raw} \quad (26)$$

The impact resistance is typically calculated per width of the specimens. Due to the variance in thicknesses of the tested samples, a resistance over an area R_{impact} will be calculated:

$$R_{impact} = \frac{E_{CVN}}{bh} \quad (27)$$

Where

b = the width of the sample, and

h = the thickness.

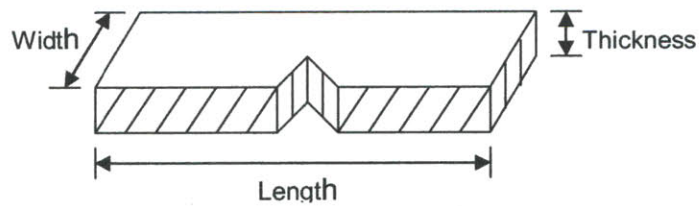


Figure 2.65 A Notched specimen for charpy test

2.4.1.3.2. Experimental Setup

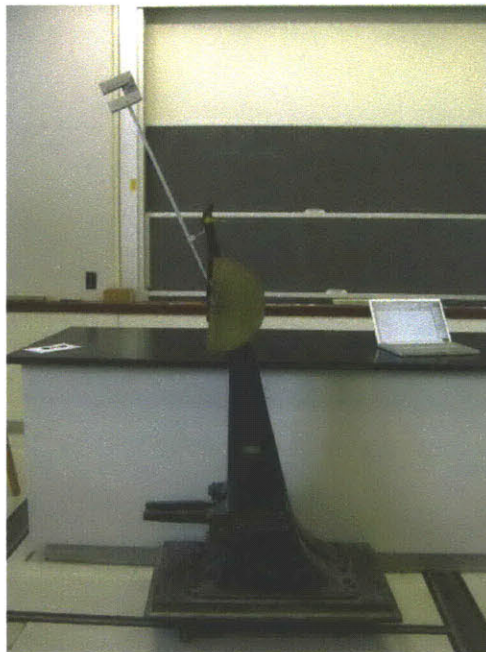


Figure 2.66 Apparatus for the charpy V-notch test

Specimens

The specimens are required to be made with a milled notch. The notch on the specimen produces a stress concentration which promotes a brittle, rather than a ductile fracture[22]. This test should be run with the specimens that have the same width. However, in this study, the three groups with different width of specimens are tested: $\frac{1}{4}$ "

$\frac{1}{2}$ " and $\frac{3}{4}$ " in order to obtain more precise results for the same composite specimens with different width.

From the bending test, we could obtain the strongest core cork combinations: biggest+ finest+ short fiber. Therefore, other combinations are eliminated to be tested because we are looking for the strong and stiff composites for a rotor blade.

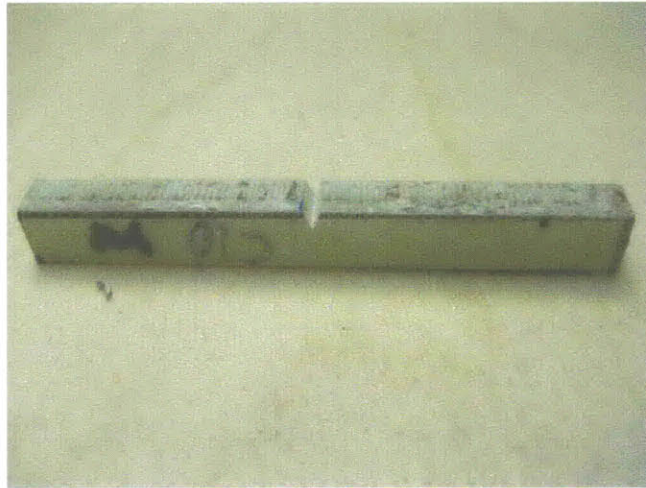


Figure 2.67 A V-notched specimen for charpy test

2.4.1.3.3. Results and Analysis

The results from the cork composites and fiberglass are shown the tables below.

	Density [Mg/ m ³]	Impact resistance per thickness [kJ/ m ²]
Pure Cork	0.58	7.68
Cork with short fibers	0.67	8.73
One-sided cork	0.69	13.63
Sandwiched cork	0.73	14.88
One-sided fiberglass	1.32	54.89
Sandwiched fiberglass	1.36	64.77

Table 2.9 The impact resistance per thickness of specimens

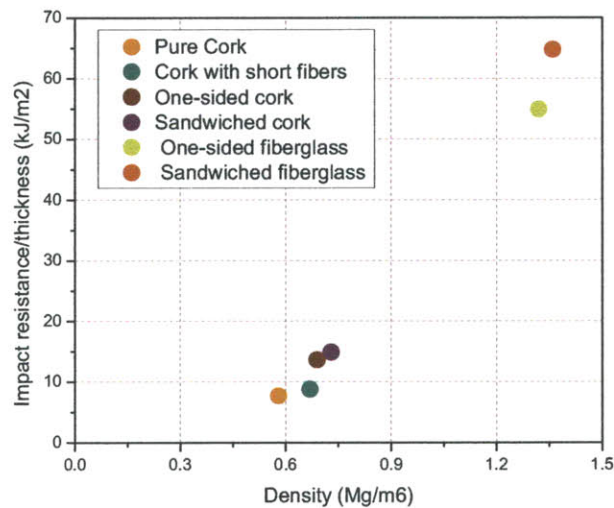


Figure 2.68 The density versus impact resistance

The charpy V-notch test determines the amount of energy absorbed by a material during fracture, i.e. amount of energy need to break a material[21]. The given material's toughness can be measured from this absorbed amount of energy, because toughness itself means the resistance to fracture of a material when it is stressed. However, one of the main disadvantages is that all results from this test are only comparative. Figure 2.68 shows that how much energy is needed to break each sample with all different density

comparatively. Toughness is the ability to absorb energy up to failure whose dimension is joules per cubic meter, so the area underneath the stress- strain curve can be represented the toughness[23].

$$\frac{\text{energy}}{\text{volume}} = \int_0^{\varepsilon_f} \sigma d\varepsilon \quad (28)$$

Where,

ε = strain

ε_f = strain upon failure, and

σ = stress

In general strength indicates how much force a material support, while toughness indicates how much energy a material absorb before rupture[23].

	Density [Mg/ m ³]	Toughness [kJ/ m ³]
Pure Cork	0.58	134.44
Cork with short fibers	0.67	149.57
One-sided cork	0.69	242.78
Sandwiched cork	0.73	266.79
One-sided fiberglass	1.32	963.68
Sandwiched fiberglass	1.36	1096.50

Table 2.10 The toughness of specimens

Table 2.10 shows the toughness of each sample from the charpy v-notch test. These results are bit different with the calculation from real strain-stress curve.

2.4.1.4. Conclusion

In summary, cork composite in a sandwich panel has shown their strength almost as same as natural woods which are used for wind turbine material due to its good fatigue property. Therefore we could confirm that cork composite can be used as a possible material for rotor blades in terms of strength.

2.4.2. Damping Properties

2.4.2.1 Sound attenuation

2.4.2.1.1. Background Theory

Sound is what the human ear hears and noise is unwanted sound. Sound is generated by all vibrating objects and propagates through the air and reaches the human ear. Sound is a variation in pressure in the region nearby to the ear. If sound becomes uncomfortable or annoying, it means that the variations in air pressure near the ear have reached too high amplitude[24].

$$dB = 10 \log_{10} \left(\frac{A_1^2}{A_0^2} \right) = 20 \log_{10} \left(\frac{A_1}{A_0} \right) \quad (29)$$

Where,

A_1 = measured amplitude, and

A_0 = reference amplitude

Due to wide range of human ear the decibel (dB) is devised to express all sound levels. The dB is a logarithmic unit of measurement because the ratio of the softest sound that human can detect and the loudest sound without damaging on ear is 1: 10^6 . Since it expresses a ratio of two quantities with the same unit, it is a dimensionless unit. By using

a base 10 logarithmic scale, the range of dB that human can hear without health threatens is from 0 dB (threshold of normal hearing) to 140 dB (the threshold of pain). However, there exists some specific ranges of frequencies that human hear very sensitively, because human ear is not equally sensitive to all the frequencies of sound within the entire spectrum. Figure 2.69 shows the various noise levels.

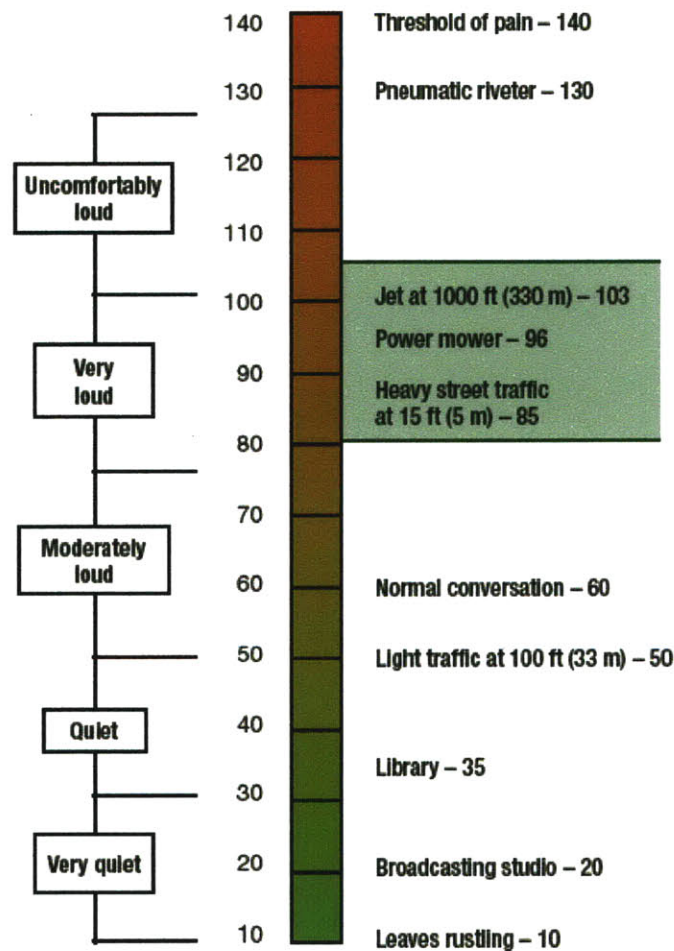


Figure 2.69 Noise levels of various sounds [24]

2.4.2.1.1. Experimental Setup

Apparatus

The sound property of samples including intensity and frequency is measured in the sound attenuation booth by hitting samples once and recorded by Amadeus II. The generated sound is measured by Amadeus system II and the distance between the record system and the origin of sound is 20cm. The recorded sound is analyzed with PRAAT program.



Figure 2.70 The apparatus for sound attenuation test in the booth

Specimens

Core cork w/without fibers and fiberglass samples are cut into the same size (10cm x 10cm x 0.5cm) in order to control undesirable effects which can be triggered by different size of samples.

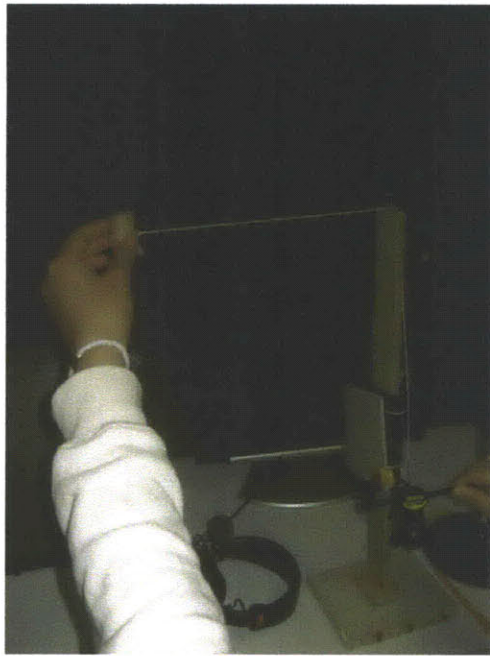


Figure 2.71 The apparatus to make sound by hitting a sample with a wood piece

2.4.2.1.3 Results and Analysis

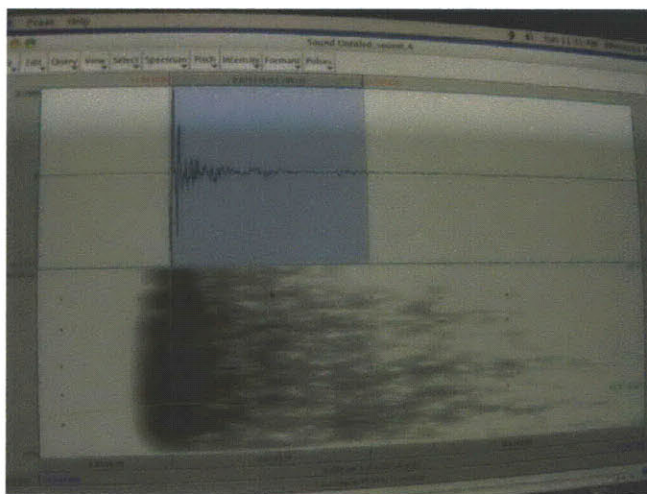


Figure 2.72 PRAAT program to analyze the sound property

When each sample is hit by a wood piece from 90 degree, which will give each sample the same amount of energy, they produce the different sounds properties. Peak and the time taken for produced sound to disappear in a sequence from high frequency are shown. Each sample is hit 3 times and results show the average.

	Pure cork core	Cork core with fibers	Fiberglass core
EI [N m ²]	0.19	0.40	1.61
Peak(dB)	63	68	76
Time (> 10,000Hz) [second]	0.025	0.028	0.02
Time(>5,000Hz) [second]	0.039	0.049	0.038
Total time[second]	0.052	0.057	0.050

Table 2.11 The results from the sound attenuation test

As seen above, fiberglass produces the loudest sound, since fiberglass releases more energy in the form of sound when it is hit. That is because it dampens less than cork composites do which means it stores less energy than cork composites. However, the time taken for sound to be disappeared is slightly less than the time taken for cork composites.

2.4.2.2. Dynamic Mechanical Analysis (DMA)

2.4.2.2.1 Background Theory

Failure modes in material such as fatigue, creep rupture, excessive deformation, and environmental aging are related to the viscoelastic properties of a plastic material[25]. For measuring and understanding viscoelastic behavior of material, dynamic mechanical analysis is often used.

Most classical materials exhibit either elastic or viscous behavior as a response to the stress applied. Solid materials such as metal show the elastic responses; it deforms proportionally when a stress is applied. The deformation of body by applied stress is recoverable when the source of stress is removed because the system stores the energy and can return it to the system[25].

Viscous behavior is a characteristic of fluid, therefore the strain of the body is not recoverable. Due to the lost of energy in the system, when the stress is removed the deformation is completely retained[25].

In a perfectly elastic system the applied sinusoidal stress and the resulting sinusoidal strain will be in phase. For an ideal fluid the stress will lead the strain by 90. A viscoelastic material has some hybrid response between a perfect elastic material and an ideal fluid: the stress and strain will be out of phase by some quantity known as the phase angle commonly called delta(δ)[26].

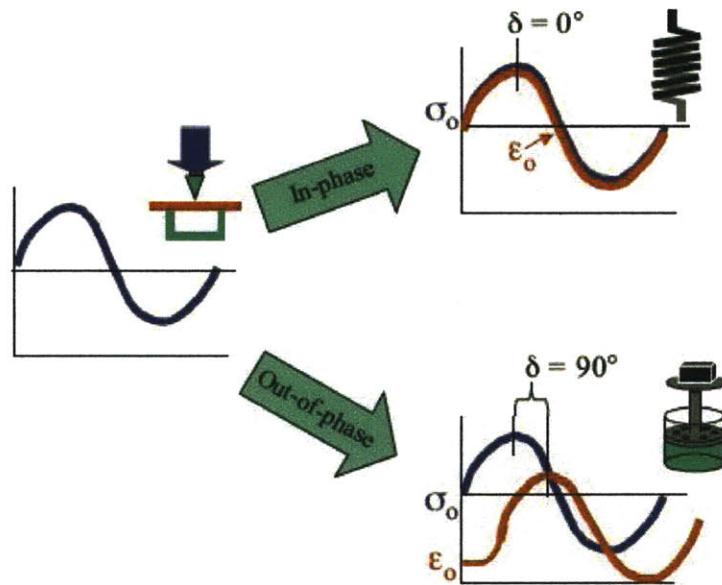


Figure 2.73 The response of a perfect elastic and viscous material for sinusoidal force [27]

In viscoelastic material a small phase angle indicates high elasticity while a large phase angle is associated with high viscous properties. The complex response of the material is resolved into the elastic or storage modulus (E') and the viscous or loss modulus (E''). When modulus is measured by traditional method, it is the complex modulus (E^*). The complex modulus can be resolved into two components; elastic modulus (E') and viscous modulus (E'')[27].

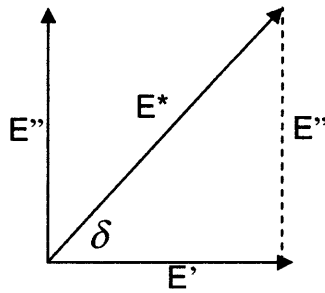


Figure 2.74 Modulus vectors [27]

The tangent of the phase angle, which is often called tan delta, is an indicator of how well the material can disperse energy or how well a material will absorb or loose energy.

$$damping = \tan \delta = \frac{E''}{E'} \quad (30)$$

High tan delta values mean that once the deformation is generated, it will not recover its origin shape because it loses more energy. Furthermore the material that has high tan delta is considered to be soft and pliable[25]. For rotor blades materials tan delta should be small because it needs strong and stiff materials.

2.4.2.2.2 Experimental Setup

Apparatus

Dynamic mechanical analysis (DMA) measures the viscoelastic properties of materials. For measuring the materials viscoelasticity, DMA Q800 dynamic mechanical analyzer is used. The method is frequency sweep with fixed temperature at 25 °C . The range of a harmonic force frequency is from 0 Hz to 200 Hz.



Figure 2.75 Dynamic mechanical analyzer Q800

Specimens

The length of specimens should be the rectangular shape with 50mm length, 10mm width and less than 7mm thickness in order to fit into the 3 point bending clamps in the testing furnace.

2.4.2.2.3 Results and Analysis

Under the considerations that the rpm of rotor blades for large wind turbine normally ranges from 30-60 rpm and 30-300 rpm for small wind turbines, the frequency range less than 100 Hz from the result is used to see the frequency dependent viscoelastic properties of specimens. Figure 2.76 shows the relationship between the tan delta and frequency from 0 Hz to 100 Hz.

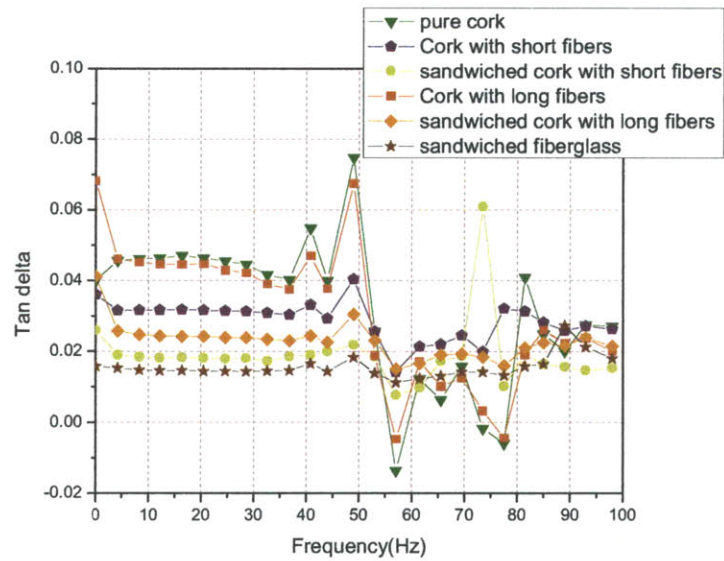


Figure 2.76 Tan delta of each samples versus frequency

Fiberglass specimen constantly shows the smallest values of tan delta over the whole frequency range, which means that fiberglass composite is the most elastic materials among the samples. Pure cork specimens and cork with long fibers composites show similar dynamic response for whole range of frequency. This might be caused by the fact that long fibers have weak bonds with cork granules in a matrix than short fibers bond with cork granules. Consequently, the dynamic properties of cork long fibers are quite similar to that of pure cork composite.

The table () is the average tan delta over the whole range of frequency and the viscous damping ratio ζ , which is the half value of tan delta[28].

	Damping	Viscous damping ratio ζ
Pure cork	0.0317	0.0158
Cork with short fibers	0.0285	0.0142
Sandwiched cork with short fibers	0.0201	0.0100
Cork with long fibers	0.0307	0.0153
Sandwiched cork with long fibers	0.0232	0.0116
Sandwiched fiberglass	0.0151	0.0075

Table 2.12 The damping and viscous damping ratio of each samples

The results is shown in the table () the damping ratio of each composites. The viscous damping ratio ξ is half of the damping. The sandwiched fiberglass has the average damping value 0.0151 at range of 0 Hz to 100 Hz which is slightly larger than the value of composites. A rotor blade experiences deformation of itself when it is operated by centrifugal and gravity force. If the rotor blades material has the relatively high tan delta, it means that the rotor blades material loses its energy to be restored from the deformation. Furthermore it could be broken if the stress on the rotor blades is applied at a high frequency for a long time because of fatigue. Pure cork composites have the highest tan delta because the only filler used in the composites is cork granules. As different fibers and skins are added to pure cork composites, the tan delta decreases, because the composites become stiffer and stronger. A sandwiched cork composite with short fibers has almost 0.02 of tan delta which is almost the equivalent system with small diameter piping system. Table 2.13 shows the viscous damping ratio ξ of other system for the comparison with other structural system. Figure 2.77 exhibits the tan delta versus density of materials. If a material has the lower density with small value of tan delta, it means that material is strong compared to its density which is desirable for rotor blades materials.

System	Viscous Damping ratio ξ
Metals (in elastic range)	<0.01
Continuous Metal Structures	0.02 to 0.04
Small Diameter Piping Systems	0.01 to 0.02
Large Diameter Piping Systems	0.02 to 0.03
Auto Shock Absorbers	≈ 0.30
Rubber	≈ 0.05
Large Buildings during Earthquakes	0.01 to 0.05
Reinforced concrete	0.05 to 0.1
Composite	0.002 to 0.003
Steel	0.001 to 0.002

Table 2.13 The viscous damping ratio of various system for comparison

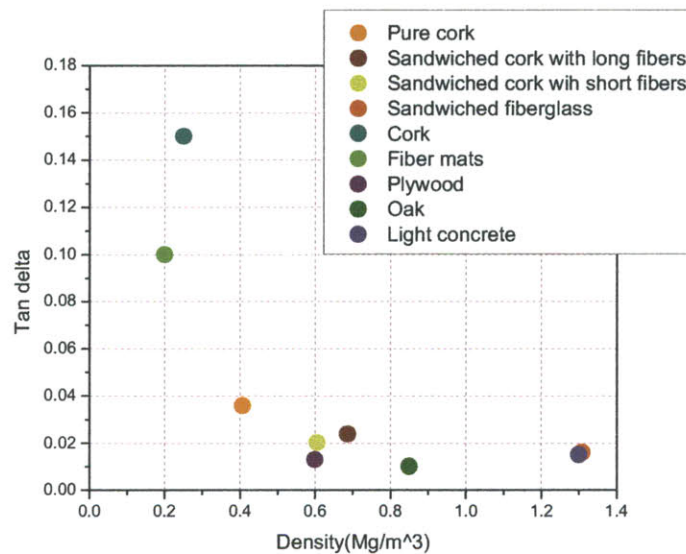


Figure 2.77 The density versus tan delta (damping) of various materials

2.4.2.3. Conclusion

Damping properties of samples are studied with two tests; sound attenuation and mechanical dynamic analysis (DMA). Cork composites produce less loud sounds when

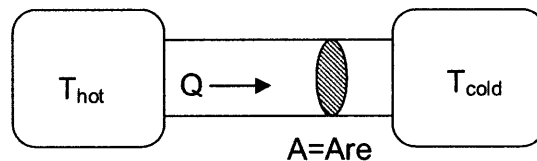
they are hit because it dampens better than fiberglass composites. This property can be checked in DMA as well. Even damping ratio of cork composites are larger than fiberglass composites which means cork composites release more energy when a force is restored in the material, this value is almost same as a small diameter piping system.

2.4.3. Isolation Properties

2.4.3.1 Thermal Conductivity

2.4.3.1.1 Background Theory

Thermal conductivity is the index of materials ability to conduct heat.



$$\Delta T = T_{\text{hot}} - T_{\text{cold}}$$

Figure 2.78 heat conduction between two heat sources

The equation(31) represents the heat conduction.

$$H = \frac{\Delta Q}{\Delta t} = kA \frac{\Delta T}{x} \quad (31)$$

Where

$\frac{\Delta Q}{\Delta t}$ = the rate of heat flow,

k = the thermal conductivity,

A = the total cross sectional area of conducting surface,

ΔT = temperature difference and

x = the thickness of conducting surface separating the 2 temperatures.

After rearranging the equation(31), the formula for thermal conductivity is obtained.

$$k = \frac{\Delta Q}{\Delta t} \frac{1}{A} \frac{x}{\Delta T} \quad (32)$$

Where

$\frac{\Delta T}{x}$ = the temperature gradient

The equation (32) can be interpreted as the quantity of heat, ΔQ , transmitted during time Δt through a thickness x , in a direction normal to a surface of area A , due to a temperature difference ΔT . It should be assumed that this takes place under steady state conditions and the heat transfer is dependent only on the temperature gradient[29]. The typical unit is W/(m·K) in SI.

2.4.3.1.2 Experimental Setup

Apparatus

The LFA 457 Microflash is used for measuring thermal conductivity of specimens. Thermal diffusivity is obtained by a short pulse of heat from laser flash which is applied to the front face of a specimen. The temperature change of the rear face is measured to calculate thermal diffusivity[30]. Thermal diffusivity α is the ratio of thermal conductivity to volumetric heat capacity. Therefore, once α is measured by LFA 457, the thermal conductivity k can be calculated.

$$\alpha = \frac{k}{\rho c_p} \quad (33)$$

Where

k = Thermal conductivity,

ρ = Density, and

C_p = Specific heat capacity

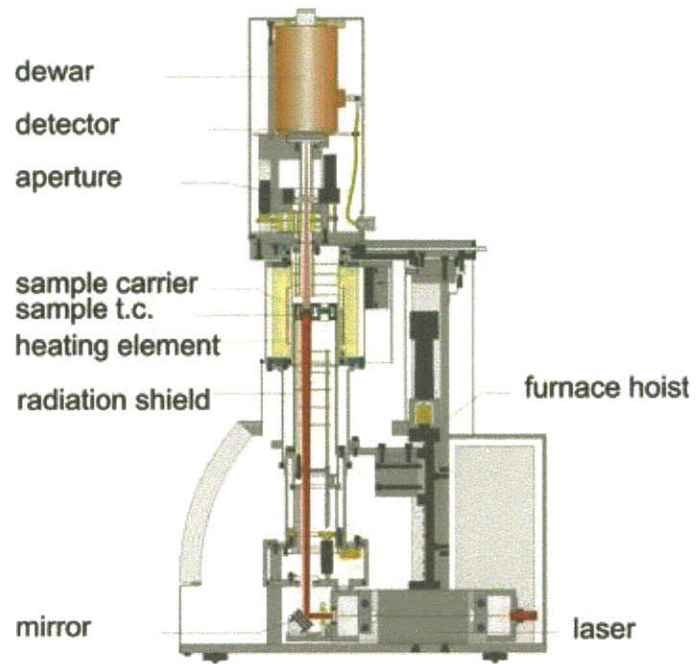


Figure 2.79 Schematic of LFA 457MicroFlash® [30]



Figure 2.80 LFA 457MicroFlash®

Specimens

The specimen size should be 2mm thickness and ½ inch diameter in order to fit in a hole of equipment furnace. After making specimen into the right size by using milling and lathe machine, it should be sprayed with liquid graphite at the same time and on the same plane with reference material. Due to the strict size for thickness of specimen in LFA (2 mm) only core materials (cork and fiberglass) are tested.



Figure 2.81 A cork specimen for thermal conductivity test



Figure 2.82 A cork specimen after graphite spraying

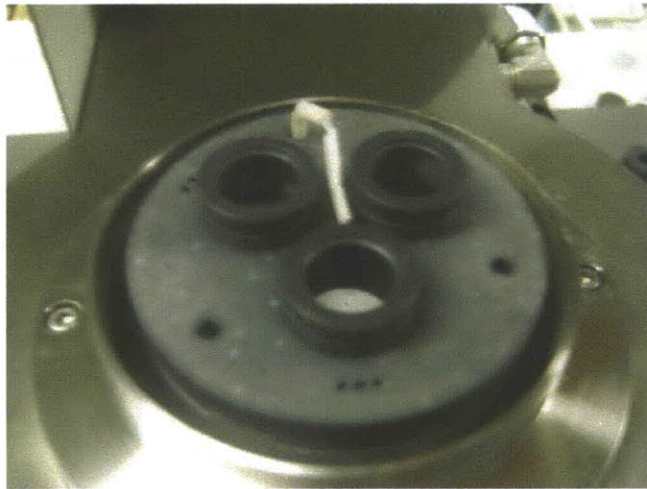


Figure 2.83 Furnace of LFA 457

2.4.3.1.3 Results and Analysis

The reference material takes one hole in the furnace and two identical specimens take other two holes. The thermal conductivity of two specimens is obtained by averaging each result from two samples at the same run. High thermal conductivity means it delivers the heat to the environments well. In other words its isolation property is not good.

	Pure cork core	Fiberglass core
Thermal conductivity(W/(m·K))	0.11	0.15

Table 2.14 The results of thermal conductivity test

From the table (), insulation materials should have the thermal conductivity values between 0.035 and 0.16. The results from the tests show that pure cork core is in this range which means this composite can be used as an insulation material.

2.4.3.2 Conclusion

Material	Thermal conductivity(W/(m·K))
Air	0.025
Wood	0.04 to 0.4
Rubber	0.016
Cork granulated	0.044
Fiberglass	0.04
Fiberglass insulating board	0.048
Epoxy	0.35
Insulation materials	0.035 to 0.16
Gold	318
Silver	429

Table 2.15 The thermal conductivity of other materials

Low/high thermal conductivity is desirable depending on the application it is used on. For the most cases on the construction of structure such as building, low thermal conductivity is desired. The rotor blade should be made of the material that has a low thermal conductivity. The result shows that good thermal character of cork core material for being a rotor blade material exhibiting even lower thermal conductivity than fiberglass samples. The theoretical thermal conductivity for both cork core and fiberglass samples can also be calculated based on the composite material theory for fiber volume ratio which are not matched to the results from the measurement.

Cork composites

$$0.6 \times 0.044 + 0.4 \times 0.35 = 0.0264 + 0.14 = 0.1664$$

Fiberglass composites

$$0.6 \times 0.04 + 0.4 \times 0.35 = 0.024 + 0.14 = 0.164$$

3. Conclusion

3.1 Summary

In order to replace the existing materials for rotor blade, cork composite in a sandwich structure has been studied. In order to find the strongest combination, parametric study is conducted. To compare the results control samples are also made by fiberglass which is mostly used as a rotor blade material. They are made by similar way of making cork composites to give the test results more validity. The static and dynamic properties of samples are determined by conducting different tests.

3.1.1 Advantages

Cork composites are strong relatively compared to its density. It has almost the same density-stiffness property with fiberglass, even though it is quite weak in terms of strength. Cork composites are made and tested in the form of a sandwich structure which is suitable for the structure requiring lightness and relatively stiffness. It also showed good isolation properties such as thermal conductivity and sound attenuation. For the dynamic property, the damping of the cork composites are almost same number as steel, which means it can store more energy rather than release it out. Storing energy is one of

critical factors in the dynamic property of materials such as rotor blades since there are forces acting on the body that make body vibrates.

3.1.2 Limitations

As mentioned before, stiffness should be over 15 GPa to become a candidate material for wind turbine. However, the strongest cork composite made for the tests has 4.7 GPa flexible modulus. The fiberglass samples have almost 2 times stronger in terms of modulus and 2 times heavier than cork composites. Both of them can move along the same line in the ashby chart which means they relatively have the same density versus modulus properties. The region where cork composites sit in the ashby chart is overlapped with the area where the modulus of wood sits. Therefore, it is possible to consider them as a possible material for wind turbine made of wood. Usually rotor blades made by wood is for smaller wind turbine whose rotor blades diameter is less than 10m. There should be more improvements in cork composites in order to compete with other leading materials.

3.2 Other Applications

The cork composites turned out to have good mechanical properties. Therefore, we could conclude that other more applications can be tried based on the cork properties studied. Usually composites materials are used in the light structure because of its excellent properties compared to its density. Especially a sandwich panel, one of composite structure, is used for the main body of boat and also air planes. The most popular sandwiched structure is honeycomb which is excellent material for constructing

airplanes. Cork composites are less strong than honeycomb and normal composites because it is formed as an agglomerate core by bonding granulated cork with resin. (particulate composite) Due to its low thermal conductivity, even less than fiberglass which is usually used as an insulator, it can be used as an insulation material.

3.3 Future Work

One of the important properties for materials experiencing repetitive structural stress is the fatigue properties. Rotor blades in wind turbine should stand more than 10^8 - 10^9 times of rotation during its life time. During the rotation it experiences structural deformation twice for each rotation because of gravity applied to slender long aspect ratio body. Therefore fatigue test should be done before making real cork rotor blades.

Once the properties of cork are excellent for a possible material for rotor blades, applications should be followed. We could check properties of cork composites that make it more useful in many applications.

Reference

1. Povl Brøndsted, Hans Lilholt, and Aage Lystrup, *Composite Materials for Wind Power Turbine Blades*, *Annu. Rev. Mater. Res.*, 2005, 35:505–38
2. Jennifer Fitzenberger, *Wind + water = untapped energy: An abundance of power exists above Earth's oceans, study finds*, *PhySorg.com*, 2009 {2}
3. Dan Ancona and Jim McVeigh, *Wind Turbine-Materials and Manufacturing Fact Sheet*, Princeton Energy Resources International, LLC, 2001
4. *Annual Report*, American Wind Energy Association, 2008
5. Karade SR, *An Investigation of Cork Cement Composites*, PhD Thesis, BCUC. Brunel University, UK, 2003
6. Helena Pereira, *Cork: biology, production and uses*, Forest Research Centre, Technical University of Lisbon, Instituto Superior de Agronomia, Portugal, 2007
7. Henrik Stiesdal, *THE WIND TURBINE COMPONENTS AND OPERATION* Bonus Energy AS, 1999
8. Wind and Hydropower Technologies program, Energy Efficiency and Renewable Energy, U.S Department of Energy, 2006, Available from http://www1.eere.energy.gov/windandhydro/wind_how.html#inside
9. *BWEA Briefing Sheet Wind Turbine Technology*, The British Wind Energy Association, 2005
10. Zbigniew Lubosny, *Wind Turbine Operation in Electric Power Systems : Advanced Modeling (Power Systems)*. Berlin: Springer, 2003.
11. The National Renewable Energy Laboratory, and a DOE national laboratory, *Small Wind Electric System*, U.S Department of Energy, Energy Efficiency and Renewable Energy, 2005
12. *Wind Turbines Energy from the Wind*, Danish Wind Industry Association, 1999
13. Ronald F. Gibson, *Principles of composite material mechanics*, Marcell Decker INC, 2007

14. *Assessment of research needs for wind turbine rotor materials technology*, National Academy Press, Washington D.C., 1991
15. Daniel Gay, Suong V. Hoa, Stephen W. Tsai, *Composite material – Design and application*, CRC Press, 2nd Edition, 2007
16. Isaac M. Daniel, Ori Ishai, *Engineering mechanics of composite materials*, Oxford University Press, 1994
17. *Core Materials in Polymeric Composites*, The A to Z of Materials, 2001.
18. Loewenstein, K.L., *The Manufacturing Technology of Continuous Glass Fibers*, New York: Elsevier Scientific. pp. 2–94, 1973
19. Chihjiun Connie Yeh, *Investigation of Cork as Filler for Fiber-reinforce Composite material in Kayaks*, Bachelor Thesis, Massachusetts Institute of Technology, USA, 2008
20. ASTM D 6110-06: Standard Test Method for Determining the Charpy Impact Resistance of Notched Specimens of Plastics, American Society for Testing and Materials Annual Book of ASTM Standards
21. Meyers and Chawla, *Mechanical Behaviors of Materials*, Prentice Hall, Inc. (Pearson Education), 1999
22. Kurishita, H et al., *Effects of V-Notch Dimensions on Charpy Impact Test Results for Differently Sized Miniature Specimens of Ferritic Steel*, *Materials Transactions, JIM (Japan)*, 34, No. 11, 1993
23. Serope Kalpakjian, *Manufacturing Process for Engineering Materials*, Pearson Education, 1998
24. Dennis Aaberg, *Generator set noise solutions: Controlling unwanted noise from on-site power system*, Power Generation Inc, 2007
25. Kevin P. Menard, *Dynamic Mechanical Analysis : a practical introduction*, Boca Raton CRC Press, 2008
26. *Dynamic Mechanical Analysis Basics: Part 1 How DMA Works*, PerkinElmer, Inc., 2007
27. M. Takemori, SPE ANTEC, 24,216, 1978
28. V. adams and A Askenazi, *Building Better Products with Finite Element Analysis*, OnWorld Press, 1999

29. David Halliday, Robert Resnick, and Jearl Walker, *Fundamentals of Physics*, John Wiley and Sons INC, 1997
30. *Thermal Diffusivity- Thermal Conductivity*, Catalogue LFA 457, NETZSCH, 2006